Resolution of ray-finned fish phylogeny and timing of diversification

Thomas J. Near[a,1], Ron I. Eytan[a], Alex Dornburg[a], Kristen L. Kuhn[a], Jon A. Moore[b], Matthew P. Davis[c], Peter C. Wainwright[d], Matt Friedman[e], and W. Leo Smith[c]

[a]Department of Ecology and Evolutionary Biology and Peabody Museum of Natural History, Yale University, New Haven, CT 06520; [b]Wilkes Honors College, Florida Atlantic University, Jupiter, FL 33458; [c]Department of Zoology, Fishes, The Field Museum, Chicago, IL 60605; [d]Department of Evolution and Ecology, University of California, Davis, CA 95616; and [e]Department of Earth Sciences, University of Oxford, Oxford OX1 3AN, United Kingdom

Edited by David M. Hillis, University of Texas, Austin, TX, and approved July 19, 2012 (received for review April 22, 2012)

Ray-finned fishes make up half of all living vertebrate species. Nearly all ray-finned fishes are teleosts, which include most commercially important fish species, several model organisms for genomics and developmental biology, and the dominant component of marine and freshwater vertebrate faunas. Despite the economic and scientific importance of ray-finned fishes, the lack of a single comprehensive phylogeny with corresponding divergence-time estimates has limited our understanding of the evolution and diversification of this radiation. Our analyses, which use multiple nuclear gene sequences in conjunction with 36 fossil age constraints, result in a well-supported phylogeny of all major ray-finned fish lineages and molecular age estimates that are generally consistent with the fossil record. This phylogeny informs three long-standing problems: specifically identifying elopomorphs (eels and tarpons) as the sister lineage of all other teleosts, providing a unique hypothesis on the radiation of early euteleosts, and offering a promising strategy for resolution of the "bush at the top of the tree" that includes percomorphs and other spiny-finned teleosts. Contrasting our divergence time estimates with studies using a single nuclear gene or whole mitochondrial genomes, we find that the former underestimates ages of the oldest ray-finned fish divergences, but the latter dramatically overestimates ages for derived teleost lineages. Our time-calibrated phylogeny reveals that much of the diversification leading to extant groups of teleosts occurred between the late Mesozoic and early Cenozoic, identifying this period as the "Second Age of Fishes."

Actinopterygii | molecular clock | species tree | Teleostei | Percomorpha

Ray-finned fishes (Actinopterygii) are one of the most successful radiations in the long evolutionary history of vertebrates, yet despite the rapid progress toward reconstructing the Vertebrate Tree of Life, only 5% of the ray-finned fish phylogeny is resolved with strong support (1). Actinopterygii contains more than 30,000 species (2), with all but 50 being teleosts (3). Compared with other large vertebrate radiations, such as mammals (4) or birds (5), a general consensus on the phylogenetic relationships and timing of diversification among the major actinopterygian and teleost lineages is lacking (3, 6, 7). This uncertainty about relationships has prevented the development of a comprehensive time-calibrated phylogeny of ray-finned fishes, which is necessary to understand macroevolutionary processes that underlie their diversity.

Most working concepts of actinopterygian relationships are based on morphological data (6, 8), and unlike other clades of vertebrates, there has been no comprehensive effort to resolve the phylogeny of actinopterygians and teleosts using molecular data that sample multiple nuclear genes and include taxa that span the major lineages. Despite the long history of using morphological data in the phylogenetics of ray-finned fishes, there are several areas of uncertainty and disagreement regarding some of the most fundamental relationships. First, there are two competing hypotheses on the phylogenetic relationships that reflect the earliest diversification of teleosts: either the Osteoglossomorpha [bony tongues (9, 10)] or Elopomorpha [eels, tarpons, and bonefish (11, 12)] are the sister lineage of all other teleosts. Second, the relationships of lower euteleosts (e.g., salmons, smelts, pikes, slickheads, and galaxiids), or "protacanthopterygians," has changed frequently as a result of phylogenetic analyses of different morphological datasets (13–15). Third, with at least 16,950 species (2), the staggering diversity of spiny-rayed fishes, and particularly percomorphs, has impeded phylogenetic resolution of this lineage, prompting Nelson (16) to label the Percomorpha as the "bush at the top of the [teleost] tree."

Applications of molecular data to these three long-standing questions in teleost phylogenetics have yielded mixed results. For example, analyses of nuclear and mtDNA gene sequences have supported all three possible relationships among osteoglossomorphs, elopomorphs, and all other teleosts [i.e., clupeocephalans (17–20)]. Molecular phylogenies have agreed with morphological inferences that "protacanthopterygians" are not monophyletic (8, 13, 14, 19, 21, 22); however, molecular inferences resolve relationships, such as a clade containing salmonids (salmon and trouts) and esociforms (pikes and mudminnows) (21–23), which are not supported in analyses of most morphological datasets (13, 14). Investigations of percomorph phylogeny using molecular data have resulted in the exciting discovery of new clades, such as monophyly of tetraodontiforms (pufferfishes) plus lophiiforms (anglerfishes) (19, 24), and the resolution of an inclusive clade of more than 4,800 species, containing cichlids, atherinomorphs (silversides), blennioids (blennies), pomacentrids (damselfishes), embiotocids (surfperches), mugilids (mullets), and other less known lineages (25). However, molecular phylogenetic analyses that have sampled the most broadly among the disparate lineages of Percomorpha have not resulted in strongly supported resolution of the deepest nodes in the clade (19, 26, 27).

Resolution of phylogenetic relationships of teleosts is critical to understanding the timing of their diversification. Currently there is discordance between the estimated age of divergence for teleosts, as inferred from the fossil record and molecular studies. Fossils of four of the earliest teleost lineages (Elopomorpha, Osteoglossomorpha, Clupeiformes, and Ostariophysi), as well as stem-lineage euteleosts (e.g., †*Leptolepides*, † = an extinct taxon) appear in a very short time interval between the Late Jurassic and Early Cretaceous (11). In contrast, molecular and genomic inferences consistently indicate that there may be a gap in the fossil record of crown-lineage teleosts, as the age estimates for

Author contributions: T.J.N., R.I.E., A.D., J.A.M., M.P.D., P.C.W., M.F., and W.L.S. designed research; T.J.N., R.I.E., A.D., K.L.K., P.C.W., M.F., and W.L.S. performed research; T.J.N., R.I.E., A.D., M.F., and W.L.S. analyzed data; and T.J.N., R.I.E., A.D., J.A.M., P.C.W., M.F., and W.L.S. wrote the paper.

The authors declare no conflict of interest.

This article is a PNAS Direct Submission.

Data deposition: The sequence reported in this paper has been deposited in the GenBank database (accession no. JX190073–JX191369).

[1]To whom correspondence should be addressed. E-mail: thomas.near@yale.edu.

This article contains supporting information online at www.pnas.org/lookup/suppl/doi:10.1073/pnas.1206625109/-/DCSupplemental.

the most recent common ancestor of living teleosts range from 310 to 350 Ma based on whole mtDNA genome sequences (28), ~320 Ma based on comparisons of paralogous gene copies resulting from the teleost whole-genome duplication (WGD) event (29), and 173–260 Ma based on fossil-calibrated nuclear gene phylogenies (7, 19, 20). Although these studies estimated ages for the crown teleost clade that are older than the fossil record, molecular age estimates across ray-finned fish lineages include those that are older, as well as younger, than fossil-based estimates. For example, the fossil record implies an origin of crown-lineage actinopterygians in the Devonian, ~385 Ma (30). However, relaxed-molecular clock analyses of a single nuclear gene resulted in an age that is younger (299 Ma) than the so-called Devonian "Age of Fishes" [416–359 Ma (19, 20)]. Discordance between these molecular and fossil age estimates, along with uncertainty in the phylogeny, contribute to a lack of understanding of this fundamental aspect of vertebrate evolution.

We investigated phylogenetic relationships and divergence times of all major lineages of Actinopterygii and Teleostei using DNA sequences of nine unlinked protein-coding nuclear genes sampled from 232 species. We used 36 well-justified absolute time calibrations from the fossil record of ray-finned fishes in relaxed-molecular clock analyses to estimate divergence times. Phylogenies resulting from these analyses were well resolved, the majority of phylogenetic inferences were supported with strong node support values, were robust to inferences using new "species tree" methods, and provide a comprehensive molecular perspective on areas of long-standing disagreement and uncertainty in the relationships of teleost fishes. Divergence times estimated from relaxed-molecular clock analyses yield a comprehensive time-scale of actinopterygian diversification that is remarkably close to ages inferred from the fossil record.

Results and Discussion

Maximum-likelihood analyses of the nine nuclear gene dataset resolved 89% of the 232 nodes in the actinopterygian phylogeny with bootstrap replicate scores (BS) ≥70% and the phylogenies inferred using the Bayesian method had 91% of the nodes strongly supported posterior probabilities (BPP) ≥ 0.95 (Fig. 1, and Figs. S1 and S2). Relationships of nonteleostean actinopterygians were consistent with traditional morphologically-based inferences (6) with polypterids (bichirs and ropefish) resolved as the sister lineage of all other actinopterygians (Actinopteri) in the relaxed-clock analysis (Fig. 1). In addition, Acipenseriformes (sturgeons and paddlefishes) were the sister lineage of Neopterygii with strong support (BS = 100%, BPP = 1.00), and Holostei (bowfin and gars) was resolved as the sister lineage of teleosts [BS = 100%, BPP = 1.00 (Fig. 1, and Figs. S1 and S2)]. These results contrast with earlier molecular studies that either resolved acipenseriforms and holosteans as an "ancient-fish" clade (31) or acipenseriforms and polypteriforms as a weakly supported clade (32).

Our results provide resolution to three of the most compelling questions in teleost phylogenetics. The molecular phylogeny resulted in the strongly supported position (BS = 97%, BPP = 1.00) of elopomorphs as the sister lineage of all other teleosts (Fig. 1, and Figs. S1 and S2). This result is also strongly supported in a species tree analysis, which accounts for potential discordance among individual gene histories, with a bootstrap proportion of 100% (Fig. S3). Evidence for Osteoglossomorpha as the sister lineage of all other teleosts was based on the presence of a single character state in the caudal fin skeleton (9, 10). On the other hand, the hypothesis that Elopomorpha is the sister lineage of all other teleosts was based on eight derived character-state changes identified from optimization of a matrix containing 135 discretely coded morphological characters (11). Our results strongly support the latter hypothesis, illustrating agreement between phylogenetic inferences from a robust morphological data matrix and our densely sampled nuclear gene DNA sequence dataset.

With regard to the relationships of early euteleosts, our phylogenetic analyses support several results from previous molecular studies and a new result that places Galaxiidae as the sister lineage of Neoteleostei (without stomiiforms) [BS = 95%, BPP = 1.00 (Fig. 1, and Figs. S1 and S2)]. Lineages previously treated as "protacanthopterygians" (3) are polyphyletic in the molecular phylogeny because the alepocephaliforms (slickheads) are resolved in a clade containing clupeomorphs (anchovies and herrings) and ostariophysians (catfish and minnows) [BS = 94%, BPP = 1.00 (21, 33)], the enigmatic freshwater Australian species *Lepidogalaxias salamandroides* is the sister lineage to all other Euteleostei (15, 23) [BS = 100%, BPP = 1.00 (Fig. 1, and Figs. S1 and S2)], salmonids (trouts and salmon) and esociforms (pikes and mudminnows) are resolved as a clade [BS = 100%, BPP = 1.00 (21, 23)], and there is strong support for a clade containing stomiiforms (dragonfishes), osmeriforms (smelts), and retropinnids (southern smelts) [BS = 100%, BPP = 1.00 (23)]. Although most of these relationships were reflected in the species tree, *Lepidogalaxias* was resolved as the sister lineage of Galaxiidae (Fig. S3). However, only one of the two gene trees (*rag1*) that sampled both *Lepidogalaxias* and Galaxiidae resolved these lineages as sharing a common ancestor. The phylogenetic resolution of these early euteleost lineages using morphology is thought to have been hampered by a mosaic of highly modified and ancestral character states (3, 13). The relationships inferred in our trees provide a phylogenetic framework to investigate the evolution of morphological character state changes, which have proven difficult to use in the inference of relationships among early diverging euteleost lineages (e.g., ref. 34).

One of the most important problems in vertebrate phylogenetics is the resolution of the major lineages of Percomorpha. The phylogeny confirms several results presented in previous molecular analyses, including the resolution of ophidiiforms (cusk eels) and batrachoidids (toadfish) as early diverging percomorphs (25, 26), a clade containing tetraodontiforms and lophiiforms (19, 24), a clade dominated by percomorphs with demersal eggs that includes cichlids, pomacentrids, blennies, ricefishes, and silversides (Atherinomorpha) (25), and the revised placement of sticklebacks with scorpionfishes, eelpouts, and perches (Perciformes) rather than their historical placement with seahorses (24–27, 35). Our molecular phylogeny provides substantial resolution and node support for the deepest percomorph relationships (Fig. 1, and Figs. S1 and S2). The degree of resolution in our phylogeny among the earliest diverging percomorphs is encouraging, and holds promise that increased taxon sampling for these molecular markers will result in the phylogenetic resolution of both the deepest and the most apical nodes in the "bush on the top of the tree" that has long vexed vertebrate biologists (6).

The phylogenetic resolution offered by the nine nuclear gene dataset not only has broad implications for understanding the evolutionary history of actinopterygians, but also provide the necessary basis for estimating their divergence times. Molecular age estimates from the nine nuclear genes agree with published analyses using whole mtDNA genomes for older nodes and with the *rag1* nuclear gene for younger nodes (Fig. 2*A* and Table S1), which is reflected in the proportion of fossil calibrations shared between those studies and our relaxed-clock analyses (Fig. 2*B*). This finding offers an explanation and reconciliation for several points of disagreement observed between molecular age estimates for ray-finned fishes and the fossil record. For example, we estimate a Silurian-Devonian origin of extant Actinopterygii, between 438.9 and 383.4 Ma (Fig. 2*A* and Table S1), which is consistent with the first occurrences of crown actinopterygian fishes (e.g., †*Mimipiscis toombsi*) in the fossil record (30). This finding contrasts with previous efforts using *rag1* that estimated the age of living ray-finned fishes between 337 and 284 Ma

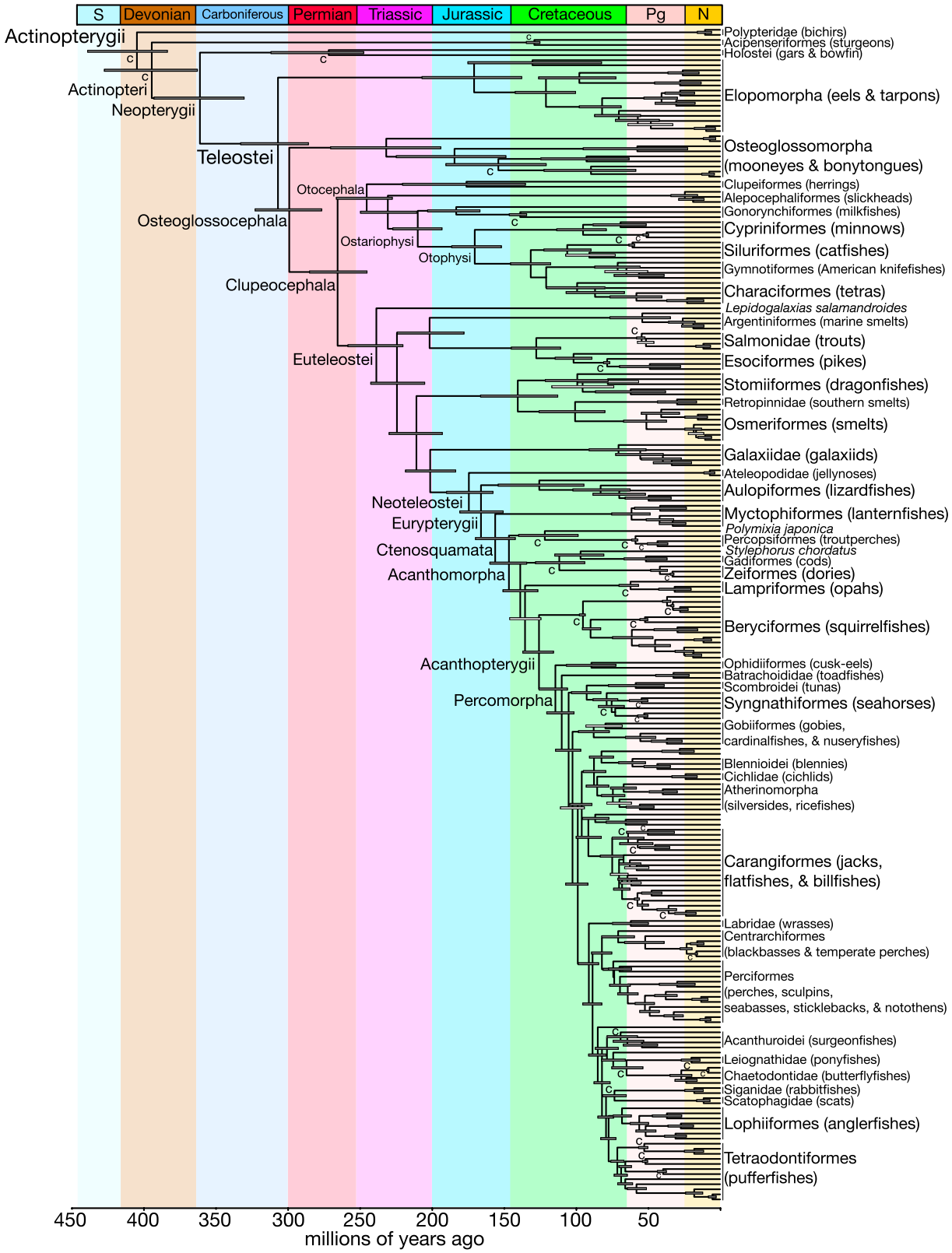

Fig. 1. Actinopterygian time-calibrated phylogeny based on nine nuclear genes and 36 fossil age constraints. Bars represent the posterior distribution of divergence-time estimates. Gray bars identify nodes supported with BPP $\geq$ 0.95, and white bars mark nodes with BPP $<$ 0.95. Nodes with age priors taken from the fossil record are marked with a "c." For full details on calibration see *Materials and Methods* and Fig. S2. The time-calibrated tree is scaled to the geological time scale with absolute time given in millions of years.

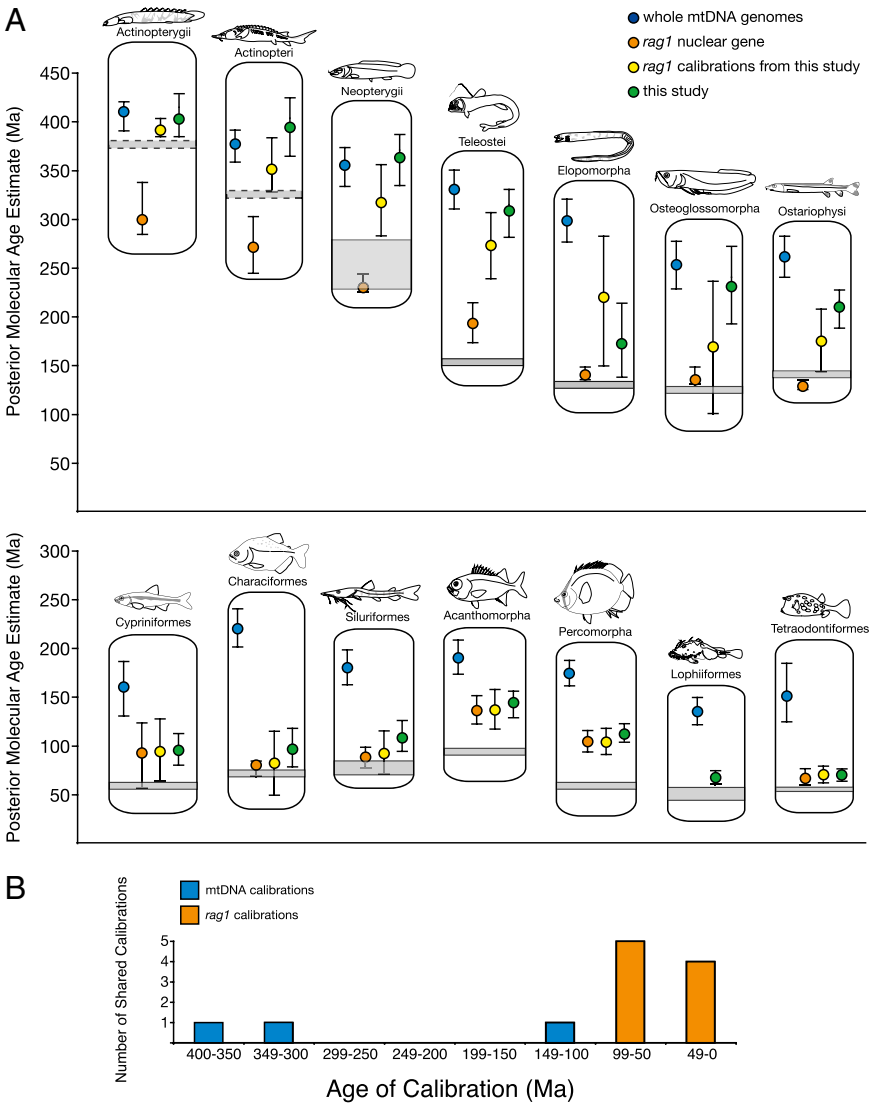

Fig. 2. Posterior distribution of molecular age estimates and patterns of calibration sharing across studies of ray-finned fish phylogeny. (*A*) Posterior distribution of molecular age estimates, in millions of years, for 14 actinopterygian lineages, resulting from analyses of whole mtDNA genomes (blue), the *rag1* nuclear gene (orange), the *rag1* nuclear gene using the calibrations from this study (yellow), and the nine nuclear gene dataset presented in this study (green). The circle represents the mean of the posterior estimate and the whiskers mark the upper and lower 95% highest posterior density of the age estimates. Gray boxes mark the oldest fossils for a given lineage, those with dashed lines were used as calibration age priors (see *Materials and Methods*) and those with solid black lines were not used as age calibrations. Line drawings of ray-finned fish species are based on photographs of specimens housed at the Peabody Museum of Natural History, Yale University, New Haven, CT. (*B*) Frequency of calibrations shared between this study and those using whole mtDNA genomes (blue) and the *rag1* nuclear gene (orange) binned by the age of the fossil calibration in millions of years (Ma).

in the Carboniferous-Permian [Fig. 2*A* (19, 20)]. This discrepancy is likely because of the use of the putative neopterygian †*Brachydegma caelatum*, which dates to the Early Permian (Artinskian-Sakmarian boundary) ~284 Ma (7), as a minimal age calibration for the crown actinopterygian clade in the *rag1*-based studies (19, 20). Using the same *rag1* gene with our calibration strategy, we estimated the age of ray-finned fishes between 402.3 and 384.3 Ma in the Devonian (Fig. 2*A*). Similarly, discrepancies between our molecular age estimates and those obtained from whole mtDNA genome analyses may be because of the use of entirely different sets of fossil calibrations that are younger than 100 Ma (Fig. 2*B*), and their application of biogeographic calibrations that constrain the ages of the derived percomorph lineage Cichlidae to correspond with specific events in the fragmentation of Gondwana that range between the Late Jurassic and Late Cretaceous [145–85 Ma (28)].

In general, published molecular age estimates for derived teleost lineages using whole mtDNA genomes are much older than the known fossils for these clades, implying the existence of substantial gaps in the fossil record that often exceed 100 Ma [Fig. 2*A* (28, 36)]. However, our molecular age estimates reject the necessity for invoking such temporally large gaps in the geological record, as our age inferences are much closer to the fossil age estimates (Fig. 2*A* and Table S1). For example, the published mtDNA age estimate for crown tetraodontiforms (pufferfishes and relatives) span the Cretaceous and Jurassic between 184 and 124 Ma (37), but the earliest definitive fossils assigned to this lineage are from Paleogene deposits in the late Paleocene (Thanetian) ~59–56 Ma (38). The lower bound of our age estimate for crown tetraodontiforms is less than 10 Ma older than these earliest fossils (Fig. 2*A* and Table S1). The same pattern of substantial difference between our age estimates and those using whole

mtDNA genome sequences was observed for the most recent common ancestors of Cypriniformes (minnows), Characiformes (piranhas and tetras), Siluriformes (catfishes), Acanthomorpha (spiny-rayed fishes), Percomorpha (perch-like fishes), and Lophiiformes (anglerfishes), with our estimates being much closer to the oldest known fossils of these lineages (Fig. 2*A* and Table S1). We obtained these results without using any of the fossil ages for these younger lineages as calibrations in our study.

The reconciliation of molecular divergence time estimates with ages implied by the fossil record allows us to investigate the age of teleosts, which has proven difficult to infer using paleontological information (11). We estimated that crown lineage teleosts first diverged during the Carboniferous to early Permian (Fig. 2*A*) (333.0–285.8 Ma), following the Devonian Age of Fishes. This estimate agrees with analyses of whole mtDNA genomes (28) and the assessment of a WGD event occurring in teleosts (29). The credibility of teleosts diversifying in the Paleozoic was challenged by analyses of the *rag1* nuclear gene that estimated teleosts diversified during the Late Triassic to Middle Jurassic (20). However, when we analyzed the *rag1* locus using the set of calibrations presented in this study, the age of teleosts shifted nearly 100 Ma, ranging from the Carboniferous to Early Triassic (305.6–237.3 Ma) (Fig. 2*A*). A Paleozoic origin for crown teleosts differs considerably from estimates based on paleontological data. The earliest fossil representatives of the teleost crown are Late Jurassic elopomorphs and ostariophysians, and these are preceded by a series of stem-teleost clades that appear between the Late Triassic and Middle Jurassic, and in roughly the temporal sequence dictated by phylogeny (11). If our molecular age estimates are accurate, then the first 100 million years of crown-teleost history is absent from the fossil record. This "teleost gap" has been noted in previous relaxed-molecular clock studies, which have attributed this discrepancy to a relatively poor record of ray-finned fishes in the latest Paleozoic (7). When taken together, our molecular age estimates, those of mtDNA based inferences, as well as the "genomic fossils" in the form of the WGD event, imply a missing record of crown teleost fossils from the Permo-Carboniferous to Middle Jurassic. We suggest that additional systematic work is needed on fossil fishes from this stratigraphic interval. If this gap in the teleost fossil record is genuine, it may be a direct consequence of a lack of suitable fossil deposits. The nearly 70-million-year span between the mid-Carboniferous and earliest Triassic is characterized by a paucity of species-rich fish *Lagerstätten* (exceptional fossil deposits yielding abundant articulated material), with existing sites of this age subject to comparatively little research (39). We hope that the recurring disagreement between timescales for the emergence of crown teleosts based on molecular and fossil datasets will encourage renewed paleontological research on this critical stratigraphic interval.

Despite the apparent gap in the fossil record for early crown–group teleosts, we find that most major teleost lineages originated in a period spanning the late Mesozoic into the early Cenozoic (Figs. 1 and 2*A*), which corresponds to patterns apparent in the fossil record (39). We identify this interval as the "Second Age of Fishes." The Devonian Age of Fishes is characterized by the presence of all major vertebrate lineages referred to as "fishes," both living and extinct [e.g., ostracoderms, placoderms, acanthodians, chondrichthyans, and so forth (40)]. Although this period in time appears to mark the origin of crown Actinopterygii (Figs. 1 and 2*A*), it does not correspond to the divergence of the major lineages that comprise the bulk of living actinopterygian biodiversity. Instead, the Second Age of Fishes represents the interval in geologic time where these species-rich lineages (e.g., otophysians and acanthomorphs) originated and eventually flourished, becoming the dominant vertebrate component of marine and freshwater habitats.

Ray-finned fishes include half of the entire species richness of vertebrates (2, 3), but had ranked last, by a wide margin, in the degree of phylogenetic resolution offered by available DNA sequence and genomic resources (1). Our phylogeny, based on a multilocus dataset, provides robust resolution and strong support across all major lineages of ray-finned fishes and teleosts. Additionally, our divergence time estimates reconcile inferences from paleontology with those obtained from other studies that used molecular methods, providing a molecular time scale that is more consistent with ages implied by the fossil record. This comprehensive molecular perspective on the evolutionary diversification of one-half of all vertebrate species provides DNA sequence data and calibration information from which to integrate resolution of clades at lower taxonomic levels (e.g., families) and estimate ages of actinopterygian lineages that lack a fossil record.

Materials and Methods

Collection of DNA Sequence Data and Phylogenetic Analyses. Standard phenol-chloroform extraction protocol or Qiagen DNeasy Blood and Tissue kits were used to isolate DNA from tissue biopsies sampled from 232 ray-finned fish species (Table S2). Previously published PCR primers were used to amplify and sequence an exon from each of nine nuclear genes [*Glyt*, *myh6*, *plagl2*, *Ptr*, *rag1*, *SH3PX3*, *sreb2*, *tbr1*, and *zic1* (22, 41)]. The genes were aligned by eye using the inferred amino acid sequences. No frame mutations or DNA substitutions that resulted in stop codons were observed in the aligned DNA sequences. The combined nine-gene dataset contained 7,587 base pairs.

Twenty-seven data partitions were designated that corresponded to the three separate codon positions for each of the nine genes. A GTR+G substitution model was used in a portioned maximum-likelihood analysis using the computer program RAxML 7.2.6 (42) run with the –D option. Support for nodes in the RAxML tree was assessed with a thorough bootstrap analysis (option –f i) with 1,000 replicates.

A species tree was inferred using gene tree parsimony implemented in the computer program iGTP (43). Individual gene trees estimated using RAxML were used as input files. Several rooting strategies were used. The individual gene trees were rooted using *Erpetoichthys calabaricus* or *Polypterus ornatipinnis*, except in three cases when these species were not sampled for a specific gene. In these cases the individual gene trees were rooted using *Scaphirhynchus platorynchus*, *Amia calva*, or *Atractosteus spatula*. A heuristic search using randomized hill climbing was performed to find the species tree that minimized the reconciliation cost for deep coalescence. This search was bootstrapped by performing it 100 times and bootstrap proportions for the resulting species trees were calculated using SumTrees in the DendroPy package (44).

Relaxed-Molecular Clock Analyses. Divergence times of ray-finned fish lineages were estimated using an uncorrelated lognormal (UCLN) model of molecular evolutionary rate heterogeneity implemented in the computer program BEAST v1.6.1 (45, 46). The nucleotide substitution models for the nine-gene dataset were partitioned by gene and codon as in the RAxML analysis above, but the UCLN molecular clock models were partitioned by gene. Thirty-six lognormal calibration priors from the fossil record of ray-finned fishes were used in the UCLN analyses (*SI Text*). To assess the rooting of the ray-finned fish phylogeny, the node representing the most recent common ancestor of Actinopteri was assigned a lognormal age prior and the monophyly of this clade was not enforced. Preliminary analyses resulted in monophyly of Actinopteri with a Bayesian posterior support = 1.0. A birth-death speciation prior was used for branching rates in the phylogeny. The BEAST analyses were run four times with each run consisting of 2.0×10^8 generations, sampling at every 5,000 generations. The resulting trees and log files from each of the five runs were combined using the computer program LogCombiner v1.6.1 (http://beast.bio.ed.ac.uk/LogCombiner). Convergence of model parameter values and estimated node-heights to their optimal posterior distributions was assessed by plotting the marginal posterior probabilities versus the generation state in the computer program Tracer v1.5 (http://beast.bio.ed.ac.uk/Tracer). Effective sample size (ESS) values were calculated for each parameter to ensure adequate mixing of the Markov chain Monte Carlo (ESS > 200). The posterior probability density of the combined tree and log files was summarized as a maximum clade credibility tree using TreeAnnotator v1.6.1 (http://beast.bio.ed.ac.uk/TreeAnnotator). The mean and 95% highest posterior density estimates of divergence times and the posterior probabilities of inferred clades were

visualized on the using the computer program FigTree v1.3.1 (http://beast.bio.ed.ac.uk/FigTree).

Fossil Calibration Age Priors. For each fossil calibration prior, we identify the calibrated node in the ray-fin fish phylogeny, list the taxa that represent the first occurrence of the lineage in the fossil record, describe the character states that justify the phylogenetic placement of the fossil taxon, provide information on the stratigraphy of the rock formations bearing the fossil, give the absolute age estimate for the fossil, outline the prior age setting in the BEAST relaxed-clock analysis, and provide any additional notes on the calibration (*SI Text*). Each calibration is numbered and the phylogenetic placement of the calibration is highlighted in Fig. S2.

ACKNOWLEDGMENTS. We thank T.-Y. Cheng and K.-T. Shao of the Biodiversity Research Museum, Academia Sinica; J. Friel of the Cornell University Museum of Vertebrates; P. A. Hastings and H. J. Walker of the Scripps Institution of Oceanography; K. P. Maslenikov and T. W. Pietsch of the Burke Museum of Natural History and Culture, University of Washington; and A. C. Bentley and E. O. Wiley of the Biodiversity Institute of the University of Kansas for generous gifts of tissue specimens. J. S. Albert, J. W. Armbruster, L. Bernatchez, T. M. Berra, C. P. Burridge, C. D. Hulsey, S. Lavoué, J. G. Lundberg, M. Miya, N. Merret, P. J. Unmack, K. Watanabe, J. M. Waters provided additional specimens; C. M. Bossu, R. C. Harrington, P. R. Hollingsworth, C. D. Hulsey, B. P. Keck, and the staff of the Carribean Research Management of Biodiversity biological research station in Curaçao provided assistance in sampling expeditions; Gregory Watkins-Colwell assisted with museum collections. K. L. Ilves provided insight on taxon sampling. This research was supported by the Peabody Museum of Natural History and National Science Foundation Grants DEB-0444842, DEB-0716155, DEB-0717009, DEB-0732642, ANT-0839007, DEB-1060869, DEB-1061806, and DEB-1061981 (to W.L.S., P.C.W., and T.J.N.); and Natural Environment Research Council Grant NERC NE/I005536/1 (to M.F.).

1. Thomson RC, Shaffer HB (2010) Rapid progress on the vertebrate tree of life. *BMC Biol* 8:19.
2. Eschmeyer WN, Fricke R (2012) Catalog of fishes (California Academy of Sciences, San Francisco).
3. Nelson JS (2006) *Fishes of the World* (John Wiley, Hoboken), 4th Ed.
4. Meredith RW, et al. (2011) Impacts of the Cretaceous Terrestrial Revolution and KPg extinction on mammal diversification. *Science* 334:521–524.
5. Hackett SJ, et al. (2008) A phylogenomic study of birds reveals their evolutionary history. *Science* 320:1763–1768.
6. Stiassny MLJ, Wiley EO, Johnson GD, de Carvalho MR (2004) *Assembling the Tree of Life*, eds Cracraft J, Donoghue MJ (Oxford Univ Press, New York), pp 410–429.
7. Hurley IA, et al. (2007) A new time-scale for ray-finned fish evolution. *Proc Biol Sci* 274:489–498.
8. Lauder GV, Liem KF (1983) The evolution and interrelationships of the actinopterygian fishes. *Bull Mus Comp Zool* 150:95–197.
9. Patterson C, Rosen DE (1977) Review of ichthyodectiform and other Mesozoic teleost fishes and the theory and practice of classifying fossils. *Bull Am Mus Nat Hist* 158: 85–172.
10. Patterson C (1998) Comments on basal teleosts and teleostean phylogeny, by Gloria Arratia. *Copeia* 1998:1107–1109.
11. Arratia G (1997) Basal teleosts and teleostean phylogeny. *Paleo Ichth* 7:5–168.
12. Arratia G (1998) Basal teleosts and teleostean phylogeny: Response to C. Patterson. *Copeia* 1998:1109–1113.
13. Fink WL (1984) *Ontogeny and Systematic of Fishes*, eds Moser HG, et al. (Allen Press, Lawrence, KS), pp 202–206.
14. Johnson GD, Patterson C (1996) *Interrelationships of Fishes*, eds Stiassny MLJ, Parenti LR, Johnson GD (Academic, San Diego), pp 251–332.
15. McDowall RM, Burridge CP (2011) Osteology and relationships of the southern freshwater lower euteleostean fishes. *Zoosystematics and Evolution* 87:7–185.
16. Nelson G (1989) *The Hierarch of Life*, eds Fernholm B, Bremer K, Jörnvall H (Elsevier, Amsterdam), pp 325–336.
17. Inoue JG, Miya M, Tsukamoto K, Nishida M (2001) A mitogenomic perspective on the basal teleostean phylogeny: Resolving higher-level relationships with longer DNA sequences. *Mol Phylogenet Evol* 20:275–285.
18. Lê HL, Lecointre G, Perasso R (1993) A 28S rRNA-based phylogeny of the gnathostomes: First steps in the analysis of conflict and congruence with morphologically based cladograms. *Mol Phylogenet Evol* 2:31–51.
19. Alfaro ME, et al. (2009) Nine exceptional radiations plus high turnover explain species diversity in jawed vertebrates. *Proc Natl Acad Sci USA* 106:13410–13414.
20. Santini F, Harmon LJ, Carnevale G, Alfaro ME (2009) Did genome duplication drive the origin of teleosts? A comparative study of diversification in ray-finned fishes. *BMC Evol Biol* 9:164.
21. Ishiguro NB, Miya M, Nishida M (2003) Basal euteleostean relationships: A mitogenomic perspective on the phylogenetic reality of the "Protacanthopterygii". *Mol Phylogenet Evol* 27:476–488.
22. Lopez JA, Chen WJ, Ortí G (2004) Esociform phylogeny. *Copeia* 2004:449–464.
23. Li J, et al. (2010) Phylogenetic position of the enigmatic *Lepidogalaxias salamandroides* with comment on the orders of lower euteleostean fishes. *Mol Phylogenet Evol* 57:932–936.
24. Miya M, et al. (2003) Major patterns of higher teleostean phylogenies: A new perspective based on 100 complete mitochondrial DNA sequences. *Mol Phylogenet Evol* 26:121–138.
25. Wainwright PC, et al. (2012) The evolution of pharyngognathy: A phylogenetic and functional appraisal of the pharyngeal jaw key innovation in Labroidei and beyond. *Syst Biol*, 10.1093/sysbio/sys060.
26. Li B, et al. (2009) RNF213, a new nuclear marker for acanthomorph phylogeny. *Mol Phylogenet Evol* 50:345–363.
27. Smith WL, Craig MT (2007) Casting the percomorph net widely: The importance of broad taxonomic sampling in the search for the placement of serranid and percid fishes. *Copeia* 2007:35–55.
28. Miya M, et al. (2010) Evolutionary history of anglerfishes (Teleostei: Lophiiformes): A mitogenomic perspective. *BMC Evol Biol* 10:58.
29. Vandepoele K, De Vos W, Taylor JS, Meyer A, Van de Peer Y (2004) Major events in the genome evolution of vertebrates: Paranome age and size differ considerably between ray-finned fishes and land vertebrates. *Proc Natl Acad Sci USA* 101: 1638–1643.
30. Gardiner BG (1984) The relationships of the palaeoniscid fishes, a review based on new specimens of *Mimia* and *Moythomasia* from Upper Devonian of Western Australia. *Bull Brit Mus (Nat Hist) Geol* 37:173–428.
31. Inoue JG, Miya M, Tsukamoto K, Nishida M (2003) Basal actinopterygian relationships: A mitogenomic perspective on the phylogeny of the "ancient fish". *Mol Phylogenet Evol* 26:110–120.
32. Li CH, Lu GQ, Ortí G (2008) Optimal data partitioning and a test case for ray-finned fishes (Actinopterygii) based on ten nuclear loci. *Syst Biol* 57:519–539.
33. Poulsen JY, et al. (2009) Higher and lower-level relationships of the deep-sea fish order Alepocephaliformes (Teleostei: Otocephala) inferred from whole mitogenome sequences. *Biol J Linn Soc Lond* 98:923–936.
34. Waters JM, et al. (2002) Phylogenetic placement of retropinnid fishes: Data set incongruence can be reduced by using asymmetric character state transformation costs. *Syst Biol* 51:432–449.
35. Near TJ, et al. (2012) Nuclear gene-inferred phylogenies resolve the relationships of the enigmatic Pygmy Sunfishes, *Elassoma* (Teleostei: Percomorpha). *Mol Phylogenet Evol* 63:388–395.
36. Nakatani M, Miya M, Mabuchi K, Saitoh K, Nishida M (2011) Evolutionary history of Otophysi (Teleostei), a major clade of the modern freshwater fishes: Pangaean origin and Mesozoic radiation. *BMC Evol Biol* 11:177.
37. Yamanoue Y, Miya M, Inoue JG, Matsuura K, Nishida M (2006) The mitochondrial genome of spotted green pufferfish *Tetraodon nigroviridis* (Teleostei: Tetraodontiformes) and divergence time estimation among model organisms in fishes. *Genes Genet Syst* 81:29–39.
38. Patterson C (1993) *Fossil Record 2*, ed Benton MJ (Chapman and Hall, London), pp 621–656.
39. Friedman M, Sallan LC (2012) Five hundred million years of extinction and recovery: A Phanerozoic survey of large-scale diversity patterns in fishes. *Palaeontology* 55: 707–742.
40. Janvier P (1996) *Early Vertebrates* (Oxford Univ Press, New York).
41. Li CH, Ortí G, Zhang G, Lu GQ (2007) A practical approach to phylogenomics: The phylogeny of ray-finned fish (Actinopterygii) as a case study. *BMC Evol Biol* 7:44.
42. Stamatakis A (2006) RAxML-VI-HPC: Maximum likelihood-based phylogenetic analyses with thousands of taxa and mixed models. *Bioinformatics* 22:2688–2690.
43. Chaudhary R, Bansal MS, Wehe A, Fernández-Baca D, Eulenstein O (2010) iGTP: A software package for large-scale gene tree parsimony analysis. *BMC Bioinformatics* 11:574.
44. Sukumaran J, Holder MT (2010) DendroPy: A Python library for phylogenetic computing. *Bioinformatics* 26:1569–1571.
45. Drummond AJ, Rambaut A (2007) BEAST: Bayesian evolutionary analysis by sampling trees. *BMC Evol Biol* 7:214.
46. Drummond AJ, Ho SYW, Phillips MJ, Rambaut A (2006) Relaxed phylogenetics and dating with confidence. *PLoS Biol* 4:e88.

Supporting Information

Near et al. 10.1073/pnas.1206625109

SI Text

Fossil Calibration Age Priors. For each fossil calibration prior, we identify the calibrated node in the ray-fin fish phylogeny, list the taxa that represent the first occurrence of the lineage in the fossil record, list the resolution of the fossil taxon in phylogenetic analyses (if any), describe the character states that justify the phylogenetic placement of the fossil taxon, provide information on the stratigraphy of the rock formations bearing the fossil, give the absolute age estimate for the fossil, outline the prior age setting in the BEAST relaxed-clock analysis, and provide any additional notes on the calibration. Each calibration is numbered and the phylogenetic placement of the calibration is highlighted in Fig. S2.

Calibration 1. *Node*: Crown-group Actinopterygii. *First occurrence*: †*Mimipiscis toombsi* and †*Moythomasia durgaringa*. Gogo Formation, Western Australia, Australia (1). *Resolution in phylogenetic analyses*: both †*Mimipiscis* and †*Moythomasia* are resolved as crown lineage actinopterygians, relative to *Polypterus*, in a maximum parsimony analysis of morphological characters (figure 10 in ref. 1). *Character states*: perforated proterygium; bases of marginal rays embrace propterygium; lateral cranial canal; (for †*Moythomasia* only) ascending process of the parapshenoid lining the spiracular groove (2). *Stratigraphy*: lower Frasnian, *transitans* conodont zone (3). *Absolute age estimate*: 382.5 Ma (4). *Prior setting*: a lognormal prior with the mean = 2.3 and SD = 0.8 to set 382.5 Ma as the minimal age offset and 419 Ma as the 95% soft upper bound. The upper bound is based on the age of osteichthyian †*Guiyu oneiros* that provides a minimal age estimate for the MRCA of Actinopterygii and Sarcopterygii (5) *Note*: †*Howqualepis* might represent an older crown group actinopterygian than either of our examples (1, 6). However, this taxon is known from lacustrine deposits that cannot easily be correlated to marine sequences, and is known from less satisfactory materials than either †*Moythomasia* or †*Mimipiscis*.

Calibration 2. *Node:* Crown-group Actinopteri. *First occurrence*: †*Cosmoptychius striatus*. Wardie Shales, Lower Oil Shale Group, Scotland (7). *Resolution in phylogenetic analyses*: see Coates (figure 9*C* in ref. 6). *Character states*: pituitary vein canal obliterated; unpaired myodome (6, 8). *Stratigraphy*: Asbian regional stage, but often correlated with the upper Viséan. We have applied the youngest date estimates for the regional stage rather than the slightly older estimated upper boundary for the Viséan (7, 9). *Absolute age estimate*: 325.5 Ma (10). *Prior setting*: a lognormal prior with the mean = 2.555 and SD = 0.8 to set 325.5 Ma as the minimal age offset and 373 Ma as the 95% soft upper bound. The upper bound is based on the calculation of FA_{95} following Marshall (11).

Calibration 3. *Node*: Stem-lineage Halecomorphi, dating the most recent common ancestor (MRCA) of Holostei, which is subtended by *Amia* and *Atractosteus*. *First occurrence*: †*Watsonulus eugnathoides*. Middle Sakamena Formation, Sakamena Group, Ambilombe Bay, Madagascar (12). *Resolution in phylogenetic analyses*: maximum parsimony analysis of 60 morphological characters resolves a monophyletic Holostei containing †*Watsonulus* and *Amia* (e.g., figure 3 in ref. 13). *Character states*: maxilla with posterior excavation; symplectic participates in lower jaw joint (14). *Stratigraphy*: Induan-Olenekian, ('Scythian') (15). *Absolute age estimate*: 245.9 Ma (16). *Prior setting*: a lognormal prior with the mean = 2.86 and SD = 0.8 to set 245.9 Ma as the minimal age offset and 311 Ma as the 95% soft upper bound. The upper bound is based on the age of †*Mesopoma planti* that is resolved as a stem lineage actinopteran in a maximum parsimony inferred phylogeny based on 72 morphological characters (figure 7 in ref. 17), and dated to the Kasimovian-Moscovian (Westphalian) at 311 Ma (6). *Note*: We have reexamined the type material of †*Brachydegma caelatum* (MCZ 6503), a Permian actinopterygian previously identified as a stem halecomorph and the oldest crown-group holostean and neopterygian (18). We find evidence in support of this interpretation lacking. Most notably, this taxon lacks both a maxilla that is free from (i.e., fails to contact) the preoperculum and a supramaxilla, two features that otherwise characterize neopterygians. Furthermore, we are unconvinced by the putative synapomorphies said to link †*B. caelatum* with other halecomorphs (e.g., an enlarged median gular, which is broadly distributed phylogenetically; an intended posterior margin of the maxilla, which is not apparent in †*B. caelatum*).

Calibration 4. *Node*: Stem lineage Polyodontidae, dating the MRCA of *Polyodon* and *Scaphirhynchus*. *First occurrence*: †*Protopsephurus liui*. Jianshangou beds, lower Yixian Formation, Jehol Group, Liaoning Province, China (19). *Resolution in phylogenetic analyses*: maximum parsimony analysis of 62 morphological characters resolve a clade containing the two sampled polyodontid species, *Polyodon spatula* and †*Protopsephurus liui* (figure 17 in ref. 20). *Character states*: stellate bones; long median dorsorostral and ventrorostral bones; anterior, middle and posterior divisions of fenestra longitudinalis; microctenoid scales (19). *Stratigraphy*: latest Barremian-earliest Aptian (19). *Absolute age estimate*: 124.6 Ma, as ash beds in the lower Yixian Formation have been radiometrically dated to 124.6 ± 0.2, 124.6 ± 0.3, 125.0 ± 0.18, and 125.0 ± 0.19 Ma using Argon ($^{40}Ar/^{39}Ar$) isotope ratios (21, 22). *Prior setting*: a lognormal prior with the mean = 1.948 and SD = 0.8 to set 124.6 Ma as the minimal age offset and 150.8 Ma as the 95% soft upper bound. The upper bound is based on the age of †*Peipiaosteus pani* that is from the Late Jurassic (Tithonian) and phylogenetically resolved as a stem acipenseriform (figures 17 and 23 in ref. 20).

Calibration 5. *Node*: Stem lineage Notopteridae, dating the MRCA of *Gymnarchus*, *Gnathonemus*, *Xenomystus*, and *Chitala*. *First occurrence*: †*Palaeonotopterus greenwoodi*. Kem-Kem Beds, southern Morocco (24–26). *Resolution in phylogenetic analyses*: maximum parsimony analysis of morphological characters resolve †*Palaeonotopterus* and Notopteridae as sister lineages (figure 13*A* in ref. 25). *Character states*: elongate foramen for N.V + N.VII straddling suture between prootic and pterospohenoid in orbital wall; auditory fenestra between prootic and basioccipital; saggita with prominent anterior process (25). *Stratigraphy*: uppermost Albian-lowermost Cenomanian (25, 27). *Absolute age estimate*: 99.6 Ma (28). *Prior setting*: a lognormal prior with the mean = 1.36 and SD = 0.8 to set 99.6 Ma as the minimal age offset and 114.1 Ma as the 95% soft upper bound. The upper bound is based on the calculation of FA_{95} following Marshall (11).

Calibration 6. *Node*: Stem lineage Chanidae, dating the MRCA of *Chanos* and *Cromeria*. *First occurrence*: †*Rubiesichthys gregalis*. Montsec, Lérida, Spain (29). *Resolution in phylogenetic analyses*: maximum parsimony anlaysis of 130 morphological characters results in a clade containing *Chanos*, †*Rubiesichthys*, †*Gordichthys*, †*Tharrhias*, †*Parachanos*, †*Dastilbe*, and †*Aethalionopsis* (figure 7.9 in ref. 30). *Character states*: frontals broad anteriorly; premaxilla broad with long oral process; ascending process of

premaxilla absent; high coronoid process; mandible depth greatest at midlength; mandibular notch present; quadrate/articular joint located anterior to orbit; opercular bone broad; suprapreopercular bone broad; neural arches anterior to dorsal fin autogenous; hypural one independent from first ural centrum (31, 32). *Stratigraphy*: Berriasian-Valanginian (29, 33). *Absolute age estimate*: 133.9 Ma. *Prior setting*: a lognormal prior with the mean = 1.51 and SD = 0.8 to set 133.9 Ma as the minimal age offset and 150.8 Ma as the 95% soft upper bound. The upper bound is based on the Tithonian stem-lineage ostariophysian †*Tischlingerichthys viohi* (34).

Calibration 7. *Node*: Stem lineage Ictaluridae, dating the MRCA of *Ameiurus* and *Cranoglanis*. *First occurrence*: †*Astephus* sp. Polecat Bench Formation, Cedar Point Quarry, Wyoming, United States (35). *Resolution in phylogenetic analyses*: †*Astephus* is resolved as the sister lineage of Ictaluridae in phylogenetic trees based on morphological data (figure 1 in ref. 36). *Character states*: posterior skull roof bears ridges and pitting; base of supraoccipital process broad; cranial fontanelles widely open (35). *Stratigraphy*: Selandian, chron 26r; lower Tiffanian North American Land Mammal Age (NALMA) (37). Ash bed below dated to 59.0 ± 0.30 based on laser-fusion and 59.11 ± 0.34 based on $^{40}Ar/^{39}Ar$ dating (37). *Absolute age estimate*: 59.0 Ma. *Prior setting*: a lognormal prior with the mean = 1.135 and SD = 0.8 to set 59.0 Ma as the minimal age offset and 70.6 Ma as the 95% soft upper bound. The upper bound is based on the earliest known siluriform fossils that date from the Maastrichtian and Campanian of Argentina, Bolivia, and Brazil. These fossils consist of fragmentary remains of fin spines, pectoral girdles, and neurocrania, but cannot be assigned to any of the crown-lineage Siluriformes (reviewed in ref. 38).

Calibration 8. *Node*: Stem lineage Ictiobinae, dating the MRCA of *Ictiobus* and *Hypentelium*. *First occurrence*: †*Amyzon brevipenne* and †*Amyzon aggregatum*. Allenby Formation, Pleasant Valley, British Columbia, Canada (†*A. brevipenne*); Horsefly beds, British Columbia, Canada; Green River Formation (Laney Shale Member), Fontenelle Reservoir, Wyoming, United States; Klondie Mountain Formation, Republic, Washington, United States (†*A. aggregatum*) (39, 40). *Resolution in phylogenetic analyses*: phylogenetic anlaysis of 157 morphological characters resolves †*Amyzon* as the sister lineage of a clade containing *Ictiobus* and *Carpiodes* (41: Fig. 6). *Character states*: a widely separated and robust hypohyal process, first transverse process is long, a wide and laterally elevated dermethmoid shape, five to seven large supraneurals, and the dermethmoid spine is moderate and expanded at the base (41). *Stratigraphy*: Ypresian-Lutetian or Bridgerian NALMA (40, 42, 43); Klondike Mountain Formation radiometrically dated to 49.42 ± 0.54 Ma using $^{40}Ar/^{39}Ar$ (44). *Absolute age estimate*: 49.4 Ma. *Prior setting*: a lognormal prior with the mean = 0.764 and SD = 0.8 to set 49.4 Ma as the minimal age offset and 57.0 Ma as the 95% soft upper bound. The upper bound is based on the oldest fossil remains of crown lineage cypriniforms that are isolated cleithra, similar to those of †*Amyzon*, from the Paskapoo Formation dated to the middle Thanetian (37, 45).

Calibration 9. *Node*: Stem lineage Esocidae, dating the MRCA of *Esox* and *Novumbra*. *First occurrence*: †*Estesesox foxi*. Milk River Formation, Alberta, Canada (46). *Resolution in phylogenetic analyses*: none. *Character states*: 'c'-shaped bases for depressible dentary teeth (46). *Stratigraphy*: upper Campanian, radiometrically dated between 76.4 and 78.2 Ma (47). *Absolute age estimate*: 76.4 Ma. *Prior setting*: a lognormal prior with the mean = 1.091 and SD = 0.8 to set 76.4 Ma as the minimal age offset and 87.5 Ma as the 95% soft upper bound. The upper bound is based on the calculation of FA_{95} following Marshall (11).

Calibration 10. *Node*: Stem lineage Salmoninae, dating the MRCA of *Thymallus*, *Salvelinus*, *Hucho*, and *Coregonus*. *First occurrence*: †*Eosalmo driftwoodensis*. Driftwood Creek, Allenby, and Klondike Mountain formations of British Columbia, Canada, and Washington, United States (48). *Resolution in phylogenetic analyses*: resolved as the sister lineage of Salmoninae in a maximum parsimony analysis of 54 morphological characters (48). *Character states*: small scales; posterior part of frontal expanded over autosphenotic; hyomandibular fossa on pterotic long; posterior portion of entopterygoid overlapped by metapterygoid and quadrate; premaxillary process of the maxilla extends dorsally at an angle exceeding 10°; suprapreopercle present; anterior end of preopercular canal on horizontal arm of preopercle turns anteroventrally; first uroneural expanded, forming a fan-shaped stegural (48). *Stratigraphy*: middle Ypresian, U-Pb zircon dated to 51.77 ± 0.34 Ma (49). *Absolute age estimate*: 51.8 Ma. *Prior setting*: a lognormal prior with the mean = 1.618 and SD = 0.8 to set 51.8 Ma as the minimal age offset and 76.4 Ma as the 95% soft upper bound. The upper bound is based on the age of †*Estesesox foxi* (see calibration 9).

Calibration 11. *Node*: Stem lineage Polymixiiformes, dating the MRCA of *Polymixia* and Percopsiformes (*Percopsis*, *Aphredoderus*, and *Chologaster*). *First occurrence*: †*Homonotichthys dorsalis*. Lower Chalk of Sussex and Kent, United Kingdom (50). *Resolution in phylogenetic analyses*: none. *Character states*: four full-sized branchiostegals; anterior branchiostegals reduced and forming support for chin barbel (50, 51). *Stratigraphy*: middle-upper Cenomanian, zone of *Holoaster subglobosus* (50, 52). *Absolute age estimate*: 93.6 Ma (28). *Prior setting*: a lognormal prior with the mean = 0.476 and SD = 0.8 to set 93.6 Ma as the minimal age offset and 99.6 Ma as the 95% soft upper bound. The upper bound is based on the Cenomanian aged stem-lineage acanthomorph ctenothrissiform taxa †*Aulolepis*, †*Ctenothrissa*, and †*Heterothrissa* (50, 53).

Calibration 12. *Node*: Stem lineage Percopsidae, dating the MRCA of Percopsiformes (*Percopsis*, *Aphredoderus*, and *Chologaster*). *First occurrence*: †*Massamorichthys wilsoni*. Paskapoo Formation, Joffre Bridge, Alberta, Canada (54). *Resolution in phylogenetic analyses*: maximum parsimony analysis of 47 morphological characters resolves a clade containing †*Massamorichthys*, *Percopsis*, †*Amphiplaga*, †*Erismatopterus*, and †*Lateopisciculus* (figure 2 in ref. 55). *Character states*: dorsal process of maxilla present; supraoccipital crest extends posterior to first neural spine (55). *Stratigraphy*: Thanetian, or middle Tiffanian NALMA (56). *Absolute age estimate*: 57.0 Ma (37). *Prior setting*: a lognormal prior with the mean = 0.525 and SD = 0.8 to set 57.0 Ma as the minimal age offset and 65.3 Ma as the 95% soft upper bound. The upper bound is based on the calculation of FA_{95} following Marshall (11).

Calibration 13. *Node*: Stem lineage Aphredoderidae, dating the MRCA of *Aphredoderus* and *Chologaster*. *First occurrence*: †*Trichophanes foliarum*. Florissant Formation, Colorado, United States (57). *Resolution in phylogenetic analyses*: †*Trichophanes* and *Aphredoderus* form a clade in a maximum parsimony anlaysis of 47 characters (figure 2 in ref. 55). *Character states*: ventral margins of lachrymal and infraorbitals serrate; alveolar process of premaxilla divided into separate segments (55, 57). *Stratigraphy*: upper Priabonian, radiometrically dated using $^{40}Ar/^{39}Ar$ isotope ratios to 34.07 Ma (58). *Absolute age estimate*: 34.1 Ma. *Prior setting*: a lognormal prior with the mean = 1.899 and SD = 0.8 to set 34.1 Ma as the minimal age offset and 59.0 Ma as the 95% soft upper bound. The upper bound is based on the age of the percopsid †*Massamorichthys wilsoni* (see calibration 12).

Calibration 14. *Node*: Stem lineage Zeiformes, dating the MRCA of Zeiformes (*Cyttopsis*, *Zenopsis*, and *Zeus*), Gadiformes (*Lota* and *Coryphaenoides*), and *Stylephorus chordatus*. *First occurrence*: †*Cretazeus rinaldii*. "Calcari di Melissano," Cavetta quarry, Lecce

province, Italy (59). *Resolution in phylogenetic analyses*: maximum parsimony analysis of 107 morphological characters placed †*Cretazeus* in a polytomy subtending all sampled extant zeiform species, but this clade was derived relative to the stem †*Archaeozeus* and †*Protozeus* (figure 7 in ref. 60). *Character states*: mobile palatine; dorsal- and anal-fin rays unbranched; hypurals 1–4 consolidated; metapterygoid small; paraphypural not in contact with last centrum; procumbent neural spines of posterior abdominal and anterior caudal vertebrate; one supraneural; two epurals; branchiostegals 3+4; two anal-fin spines (59). *Stratigraphy*: latest Campanian-earliest Maastrichtian (59). *Absolute age estimate*: 70.6 Ma (28). *Prior setting*: a lognormal prior with the mean = 1.016 and SD = 0.8 to set 70.6 Ma as the minimal age offset and 80.9 Ma as the 95% soft upper bound. The upper bound is based on the calculation of FA_{95} following Marshall (11). *Note*: phylogenetic analysis of 107 morphological characters that are restricted to zeiform taxa with two outgroups resolve †*Cretazeus* in a more derived position than used in this calibration age prior (figure 9 in ref. 60)

Calibration 15. *Node*: Stem lineage *Zenopsis*, dating the MRCA of *Zenopsis* and *Zeus*. *First occurrence*: †*Zenopsis clarus*, †*Zenopsis tyleri*, and †*Zenopsis hoernesi*. Lower Maikopian series, Psheka Horison of the Belaya River, Caucasus (61), and Lower Dysodylic shales, Strujinoasa-Drăguşina and Piatra Neamţ, Romania (62); Lower Dysodylic shales, Piatra Neamţ, Romania (62); Laško (Tüffer), Slovenia (62). *Resolution in phylogenetic analyses*: maximum parsimony analysis of 45 morphological characters resulted in a tree where †*Z. clarus*, †*Z. tyleri*, and †*Z. hoernesi*, and *Zenopsis oblongus* are resolved in a clade (figure 1 in ref. 63). *Character states*: slender lachrymal; pelvic-fin spines absent; buckler-like plates present along ventral midline of abdomen, and along dorsal ridge from middle of spinous to end of soft dorsal fin (63). *Stratigraphy*: lower Rupelian [P18], lower Khadumian regional stage (64). *Absolute age estimate*: 32 Ma (65). *Prior setting*: a lognormal prior with the mean = 0.231 and SD = 0.8 to set 32.0 Ma as the minimal age offset and 36.7 Ma as the 95% soft upper bound. The upper bound is based on the calculation of FA_{95} following Marshall (11).

Calibration 16. *Node*: Stem lineage Lampridae dating the MRCA of *Lampris*, *Regalecus*, and *Trachipterus*. *First occurrence*: †*Turkmene finitimus*. Danatinsk Suite, Uylya-Kushlyuk locality, Turkmenistan (66, 67). *Resolution in phylogenetic analysis*: none. *Character states*: first dorsal-fin pterygiophore strongly reclined posteriorly; enlarged pectoral fins inserting high on flank; pectoral girdle broad ventrally, with expanded coracoid; long parapophyses absent from abdominal vertebrate (67). *Stratigraphy*: uppermost Thanetian-lowermost Ypresian (68). *Absolute age estimate*: 55.8 Ma (65). *Prior setting*: a lognormal prior with the mean = 2.006 and SD = 0.8 to set 55.8 Ma as the minimal age offset and 83.5 Ma as the 95% soft upper bound. The upper bound is based on the Campanian aged veliferid †*Nardovelifer altipinnis* (69). Veliferidae is resolved as the sister lineage of all other lampriforms in morphological and molecular phylogenetic analyses (70, 71).

Calibration 17. *Node*: Stem lineage Trachichthyoidei dating the MRCA of Beryciformes. *First occurrence*: †*Hoplopteryx lewesiensis* and †*Hoplopteryx simus*. Lower Chalk of Sussex and Kent, United Kingdom (50). Resolution in phylogenetic analyses: none. *Character states*: teeth form vertical band at dentary symphysis, extending ventral to sensory canal; sclerotic ossicle unossified (51). *Stratigraphy*: middle-upper Cenomanian, zone of *Holoaster subglobosus* (50, 52). *Absolute age estimate*: 93.6 Ma (28). *Prior setting*: a lognormal prior with the mean = 0.479 and SD = 0.8 to set 93.6 Ma as the minimal age offset and 105.8 Ma as the 95% soft upper bound. The upper bound is based on the Albian aged aulopiform †*Apateodus glyphodus* from the Gault Clay Formation, United Kingdom (72).

Calibration 18. *Node*: Stem lineage Myripristinae, dating the MRCA of *Myripristis* and *Sargocentron*. *First occurrence*: †*Eoholocentrum macrocephalum*, †*Berybolcensis leptacanthus*, and †*Tenuicentrum pattersoni*. Pesciara beds of "Calcari nummulitici," Bolca, Italy (73–75). *Resolution in phylogenetic analyses*: analysis of 72 morphological characters resolve †*Eoholocentrum*, †*Berybolcensis*, and †*Tenuicentrum* as stem-lineage Myripristinae (figure 10 in ref. 76). *Character states*: tooth-bearing platform expanded and overhangs lateral side of dentary near symphysis; premaxillary tooth field curves dorsally toward ascending process at symphysis; edentulous ectopterygoid (†*Berybolcensis* and †*Tenuicentrum*); spinous procurrent caudal-fin rays reduced to four in the upper and three in the lower lobe (†*Berybolcensis* and †*Tenuicentrum*) (76). *Stratigraphy*: upper Ypresian [NP14] (77). *Absolute age estimate*: 50 Ma (65). *Prior setting*: a lognormal prior with the mean = 0.672 and SD = 0.8 to set 50.0 Ma as the minimal age offset and 57.3 Ma as the 95% soft upper bound. The upper bound is based on the calculation of FA_{95} following Marshall (11).

Calibration 19. Node: Stem lineage *Gephyroberyx* dating the MRCA of *Gephyroberyx*, *Hoplostethus*, and *Paratrachichthys sajademalensis*. *First occurrence*: †*Gephyroberyx robustus*. Lower Maikopian Series, Belaya, Malyi Zelenchuk, and Gumista rivers, Caucasus (61). Resolution in phylogenetic analyses: none. *Character states*: ventral ridge of body bears a series of scute-like scales; preopercular bears pronounced spine at posterior angle; eight dorsal-fin spines (78, 79). *Stratigraphy*: lower Rupelian [P18] lower Khadumian regional stage (64). *Absolute age estimate*: 32 Ma (65). *Prior setting*: a lognormal prior with the mean = 0.231 and SD = 0.8 to set 32.0 Ma as the minimal age offset and 36.7 Ma as the 95% soft upper bound. The upper bound is based on the calculation of FA_{95} following Marshall (11).

Calibration 20. *Node*: Crown lineage Syngnathiformes, dating the MRCA of *Fistularia*, *Syngnathus*, *Aulostomus*, *Aeoliscus*, and *Macroramphosus*. *First occurrence*: †*Gasterorhamphosus zuppichinii*. "Calcari di Melissano," Porto Selvaggio, Lecce province, Italy (80). *Resolution in phylogenetic analyses*: none, but Orr (81) argues that †*Gasterorhamphosus* is a stem lineage of a clade containing Macrorhamphosidae and Centriscidae. *Character states*: anal-fin spine absent; enlarged dorsal-fin spine with serrated posterior margin; elongated tubular snout; pleural ribs absent; cleithrum bears enlarged posterodorsal process; rod-like anteroventral process of coracoid; pectoral rays simple (81, 82). *Stratigraphy*: uppermost Campanian-lowermost Maastrichtian (83). *Absolute age estimate*: 70.6 Ma (28). *Prior setting*: a lognormal prior with the mean = 1.016 and SD = 0.8 to set 70.6 Ma as the minimal age offset and 80.9 Ma as the 95% soft upper bound. The upper bound is based on the calculation of FA_{95} following Marshall (11).

Calibration 21. Node: Stem lineage Centriscidae, dating the MRCA of Centriscidae (*Aeoliscus* and *Macroramphosus*) and *Aulostomus*. *First occurrence*: †*Paramphisile weileri* and †*Paraeoliscus robinetae*. Pesciara beds of "Calcari nummulitici," Bolca, Italy (84). *Resolution in phylogenetic analyses*: none. *Character states*: caudal fin directed posteroventrally (*Paraeoliscus*); dorsal spine jointed distally (81). *Stratigraphy*: upper Ypresian [NP14] (77). *Absolute age estimate*: 50 Ma (65). *Prior setting*: a lognormal prior with the mean = 0.672 and SD = 0.8 to set 50.0 Ma as the minimal age offset and 57.3 Ma as the 95% soft upper bound. The upper bound is based on the calculation of FA_{95} following Marshall (11).

Calibration 22. *Node*: Stem lineage Syngnathidae, dating the MRCA of *Syngnathus* and *Fistualria*. *First occurrence*: †"*Syngnathus*" *heckeli* and †*Prosolenostomus lessinii*. Pesciara beds of "Calcari nummulitici," Bolca, Italy (84). Resolution in phylogenetic analyses: none. *Character states*: greatly elongated body; body completely encircled by armoured plates; median fins greatly reduced or absent (81). *Stratigraphy*: upper Ypresian [NP14] (77). *Absolute age estimate*: 50 Ma (65). *Prior setting*: a lognormal prior with the mean = 0.672 and SD = 0.8 to set 50.0 Ma as the minimal age offset and 57.3 Ma as the 95% soft upper bound. The upper bound is based on the calculation of FA_{95} following Marshall (11).

Calibration 23. *Node*: Stem lineage Carangidae, dating the MRCA of Carangidae (*Caranx*, *Seriola*, and *Trachinotus*), *Echeneis*, *Coryphaena*, and *Rachycentron*. *First occurrence*: †*Archaeus oblongus*. Danatinsk Suite, Uylya-Kushlyuk locality, Turkmenistan (66). *Resolution in phylogenetic analyses*: none. *Character states*: broad gap between second and third anal-fin spines (85). *Stratigraphy*: uppermost Thanetian-lowermost Ypresian (68). *Absolute age estimate*: 55.8 Ma (65). *Prior setting*: a lognormal prior with the mean = 0.776 and SD = 0.8 to set 55.8 Ma as the minimal age offset and 63.9 Ma as the 95% soft upper bound. The upper bound is based on the calculation of FA_{95} following Marshall (11).

Calibration 24. *Node*: Stem lineage Echeneidae, dating the MRCA of *Echeneis*, *Coryphaena*, and *Rachycentron*. *First occurrence*: †*Opisthomyzon glaronensis* and unnamed echeneid *cf. Echeneis*. †*Opisthomyzon*, Engi Slates, Matt, Glarus province, Switzerland (86); *cf. Echeneis* "fish shales," Frauenweiler clay pit, Germany (87). *Resolution in phylogenetic analyses*: none. *Character states*: no supraneurals; multiple anal-fin pterygiophores insert anterior to first haemal spine; spinous dorsal fin modified as adhesion disk (88, 89). *Stratigraphy*: Engi slates: Rupelian, but younger than ca. 31.7 Ma as radiometric dates for underlying Taveyannaz Formation; K/Ar: 31.7 ± 1.6 and 32.4 ± 1.6 Ma; $^{40}Ar/^{39}Ar$: 31.96 ± 0.9 Ma (90, 91). *Absolute age estimate*: 30.1 Ma (92). *Prior setting*: a lognormal prior with the mean = 0.165 and SD = 0.8 to set 30.1 Ma as the minimal age offset and 34.5 Ma as the 95% soft upper bound. The upper bound is based on the calculation of FA_{95} following Marshall (11).

Calibration 25. *Node*: Stem lineage Luvaridae, dating the MRCA of *Luvarus*, *Zanclus*, and Acanthuridae (*Acanthurus* and *Naso*). *First occurrence*: †*Avitoluvarus dianae*, †*Avitoluvarus mariannae*, †*Kushlukia permira*, and †*Luvarus necopinatus*. Danatinsk Suite, Uylya-Kushlyuk locality, Turkmenistan (93). Resolution in phylogenetic analyses: maximum parsimony analysis of 50 morphological characters resolves a clade containing †*Avitoluvarus*, †*Kushlukia*, †*Luvarus necopinatus*, and *Luvarus imperialis*, which is sister to Zanclidae + Acanthuridae (figure 18 in ref. 93). *Character states*: median pterygial truss surrounding most of body; two or fewer dorsal-fin spines; no anal-fin spines; distal end of first anal-fin pterygiophore greatly elongated anteriorly; hypurals 1–4 fused; caudal fin-rays broadly overlap hypurals; pelvic fin rudimentary in adults; teeth absent or greatly reduced (93). *Stratigraphy*: uppermost Thanetian-lowermost Ypresian (68). *Absolute age estimate*: 55.8 Ma (65). *Prior setting*: a lognormal prior with the mean = 0.776 and SD = 0.8 to set 55.8 Ma as the minimal age offset and 63.9 Ma as the 95% soft upper bound. The upper bound is based on the calculation of FA_{95} following Marshall (11).

Calibration 26. *Node*: Stem lineage Siganidae, dating the MRCA of *Siganus* and Scatophagidae (*Scatophagus* and *Selenotoca*). *First occurrence*: †*Siganopygaeus rarus*. Danatinsk Suite, Uylya-Kushlyuk locality, Turkmenistan (94). *Resolution in phylogenetic analyses*: maximum parsimony analysis of 12 morphological traits resolves four Eocene and Oligocene taxa, including †*Siganopygaeus*, as stem lineage Siganidae (figure 20 in ref. 94). *Character states*: two pelvic-fin spines; seven or more anal-fin spines; 10 or fewer anal-fin rays (94). *Stratigraphy*: uppermost Thanetian-lowermost Ypresian (68). *Absolute age estimate*: 55.8 Ma (65). *Prior setting*: a lognormal prior with the mean = 0.776 and SD = 0.8 to set 55.8 Ma as the minimal age offset and 63.9 Ma as the 95% soft upper bound. The upper bound is based on the calculation of FA_{95} following Marshall (11).

Calibration 27. *Node*: MRCA of *Bothus*, *Pseudopleuronectes*, *Samariscus*, *Symphurus*, and *Heteromycteris*. *First occurrence*: †*Eobothus minimus*. Pesciara beds of "Calcari nummulitici," Bolca, Italy (95, 96). *Resolution in phylogenetic analyses*: †*Eobothus* is the sister lineage of *Citharus* (figure 2 in ref. 95). *Character states*: complete orbital asymmetry; dorsal fin extends above orbit; hook-shaped urohyal; parahypural not in articulation with pural centrum 1; long neural spine on preural centrum 2 (95). *Stratigraphy*: upper Ypresian [NP14] (77). *Absolute age estimate*: 50 Ma (65). *Prior setting*: a lognormal prior with the mean = 0.672 and SD = 0.8 to set 50 Ma as the minimal age offset and 57.3 Ma as the 95% soft upper bound. The upper bound is based on the calculation of FA_{95} following Marshall (11).

Calibration 28. *Node*: Stem lineage of Soleidae + Cynoglossidae, dating the MRCA of *Samariscus*, *Symphurus*, and *Heteromycteris*. *First occurrence*: †*Eobuglossus* and †*Turahbuglossus*. Mokkatam Formation, Gebel Turah, Egypt (97). *Resolution in phylogenetic analyses*: none. *Character states*: blind side preopercular canal terminating on ventral margin of preopercular; convex portion of blind side dentary anterior to angulo-articular (for †*Eobuglossus*). Chanet (97) argues that †*Eobuglossus* can be identified as a soleid on the basis of the geometry of the ascending process of the blind side premaxilla. We are not convinced that the state in this fossil can be meaningfully distinguished from the condition found in cynoglossids (98). *Stratigraphy*: upper Lutetian (97). *Absolute age estimate*: 40.4 Ma (65). *Prior setting*: a lognormal prior with the mean = 0.946 and SD = 0.8 to set 40.4 Ma as the minimal age offset and 50 Ma as the 95% soft upper bound. The upper bound is based on the age of †*Eobothus* (see calibration 27).

Calibration 29. *Node*: Stem lineage Bothidae, dating the MRCA of *Bothus* and *Pseudopleuronectes*. *First occurrence*: †*Oligobothus pristinus*. Lower Dysodilic shales, Piatra Neamt, Romania (99). *Resolution in phylogenetic analyses*: none. *Character states*: myorhabdoi present (99). *Stratigraphy*: upper Rupelian [NP 23] (99). *Absolute age estimate*: 30 Ma (65). *Prior setting*: a lognormal prior with the mean = 0.165 and SD = 0.8 to set 30.0 Ma as the minimal age offset and 34.4 Ma as the 95% soft upper bound. The upper bound is based on the calculation of FA_{95} following Marshall (11).

Calibration 30. *Node*: Stem lineage of Chaetodontidae, dating the MRCA of Chaetodontidae (*Chaetodon*, *Prognathodes*, *Chelmon*, and *Forcipiger*) and Leiognathidae (*Leiognathus* and *Gazza*). *First occurrence*: Chaetodontidae *cf. Chaetodon* (tholichthys-stage larva). "Fish shales," Frauenweiler clay pit, Germany (87, 92). *Resolution in phylogenetic analyses*: none. *Character states*: Larva conforms to the *Tholichthys* pattern of anatomy. *Stratigraphy*: Rupelian (92). *Absolute age estimate*: 30.1 Ma (92). *Prior setting*: a lognormal prior with the mean = 0.165 and SD = 0.8 to set 30.1 Ma as the minimal age offset and 34.5 Ma as the 95% soft upper bound. The upper bound is based on the calculation of FA_{95} following Marshall (11).

Calibration 31. Node: Stem lineage *Chaetodon*, dating the MRCA of *Chaetodon* and *Prognathodes*. *First occurrence*: †*Chaetodon*

ficheuri. Saint-Denis du Sig, Raz-el-Aïn, Les Planteurs, and Eugène, Algeria (100). *Resolution in phylogenetic analyses*: none. *Character states*: overlapping, sequential articulation between first dorsal fin pterygiophores, supraneurals, and supraoccipital crest; second infraorbital excluded from orbital margin; two sets of lateral processes on each side of first dorsal-fin pterygiophore define a clear groove; distal head of second supraneural longer than that of first supraneural (100, 101). *Stratigraphy*: Messinian (constrained between 7.12 and 5.96 Ma) (102–104). *Absolute age estimate*: 7.1 Ma. *Prior setting*: a lognormal prior with the mean = 0.1 and SD = 0.3 to set 7.1 Ma as the minimal age offset and 8.9 Ma as the 95% soft upper bound. The upper bound is based on the calculation of FA_{95} following Marshall (11).

Calibration 32. *Node*: Stem linage *Gazza*, dating the MRCA of *Gazza* and *Leiognathus*. *First occurrence*: †*Euleiognathus tottori* (initially named as species of *Leiognathus*). Iwami Formation, Tottori Group, Japan (105, 106). *Resolution in phylogenetic analyses*: none. *Character states*: long ascending processes of premaxillae; paddle-like expansions of neural and haemal spine of preural centrum 4; single supraneural; serrated anterior margins of fin spines; caniniform teeth (107). The final character is unique to *Gazza* within leiognathids (106, 108). The nesting of *Gazza* high within the leiognathid phylogeny indicates caniniform teeth are derived within the clade (107, 109). *Stratigraphy*: middle Miocene (105, 106). *Absolute age estimate*: 11.6 Ma (110). *Prior setting*: a lognormal prior with the mean = 1.602 and SD = 0.8 to set 11.6 Ma as the minimal age offset and 23.1 Ma as the 95% soft upper bound. The upper bound is based on the age of Chaetodontidae *cf Chaetodon* (see calibration 30).

Calibration 33. *Node*: Stem lineage Diodontidae, dating the MRCA of Diodontidae (*Diodon* and *Chilomycterus*) and *Tetraodon*. *First occurrence*: †*Prodiodon tenuispinus*, †*Prodiodon erinaceus*, †*Heptadiodon echinus*, and †*Zignodon fornasieroae*, Pesciara beds of "Calcari nummulitici," Bolca, Italy (111). *Resolution in phylogenetic anlayses*: maximum parsimony analysis of 219 morphological characters results in a clade containing †*P. tenuispinus*, †*P. erinaceus*, †*H. echinus*, †*Z. fornasieroae*, *Diodon holocanthus*, and *Chilomycterus schoepfi* (figure 4 in ref. 111). *Character states*: premaxillae fused along midline; dentaries fused along midline; jaws massive (111). *Stratigraphy*: upper Ypresian [NP14] (77). *Absolute age estimate*: 50 Ma (65). *Prior setting*: a lognormal prior with the mean = 0.672 and SD = 0.8 to set 50.0 Ma as the minimal age offset and 57.3 Ma as the 95% soft upper bound. The upper bound is based on the calculation of FA_{95} following Marshall (11).

Calibration 34. *Node*: Stem lineage Ostraciidae, dating the MRCA of *Rhinesomus* and *Aracana*. *First occurrence*: †*Eolactoria sorbinii*. Pesciara beds of "Calcari nummulitici," Bolca, Italy (111). *Resolution in phylogenetic anlayses*: maximum parsimony analysis of 219 morphological characters results in a clade containing †*Eolactoria*, *Acanthostracion*, and *Ostracion* (figure 4 in ref. 111). *Character states*: dermal carapace closed behind dorsal and anal fins; scale plates absent from caudal peduncle (111). *Stratigraphy*: upper Ypresian [NP14] (77). *Absolute age estimate*: 50 Ma (65). *Prior setting*: a lognormal prior with the mean = 0.847 and SD = 0.8 to set 50.0 Ma as the minimal age offset and 58.7 Ma as the 95% soft upper bound. The upper bound is based on the Thanetian aged stem balistoid †*Moclaybalistes danekrus* (112), which is resolved as the sister lineage of an inclusive clade including Ostraciidae (figure 4 in ref. 111).

Calibration 35. *Node*: Stem lineage of Balistidae, dating the MRCA of *Abalistes* and *Cantherhines*. *First occurrence*: †*Gornylistes prodigiosus*. Kuma Horizon, Krasnodar Region, Caucasus (113). *Resolution in phylogenetic anlayses*: none. *Character states*: ventral shaft of second spine-bearing dorsal pterygiophore absent; supraneural strut present between abdominal neural spine and final spine-bearing dorsal pterygiophore; four anal-fin pterygiophores anterior to the haemal spine of the third caudal vertebra (111). *Stratigraphy*: Bartonian [NP17] Kumian regional stage (64). *Absolute age estimate*: 37.2 Ma (65). *Prior setting*: a lognormal prior with the mean = 0.37 and SD = 0.8 to set 37.2 Ma as the minimal age offset and 42.6 Ma as the 95% soft upper bound. The upper bound is based on the calculation of FA_{95} following Marshall (11).

Calibration 36. *Node*: Stem lineage *Archoplites*, dating the MRCA of *Archoplites* and *Ambloplites*. *First occurrence*: †*Archoplites clarki*. Clarkia Lake Beds, locality P-33, Idaho, United States (114, 115). *Resolution in phylogenetic analyses*: none. *Character states*: teeth on endopterygoid, ectopterygoid, and posterior basibranchial; vomer with small teeth; premaxilla with short ascending process; dentary truncate; opercle weakly notched; lachrymal serrate but rounded posteriorly; three or four supraneurals; five to eight anal fin spines (114, 116). *Stratigraphy*: Langhian-Burdigalian (Barstovian NALMA), dated to 16–15.5 Ma (117, 118). *Absolute age estimate*: 15.5 Ma (117). *Prior setting*: a lognormal prior with the mean = 0.1 and SD = 0.5 to set 15.5 Ma as the minimal age offset and 17.8 Ma as the 95% soft upper bound. The upper bound is based on the calculation of FA_{95} following Marshall (11).

1. Gardiner BG, Schaeffer B (1989) Interrelationships of lower actinopterygian fishes. *Zool J Linn Soc* 97:135–187.
2. Gardiner BG, Schaeffer B, Masserie JA (2005) A review of the lower actinopterygian phylogeny. *Zool J Linn Soc* 144:511–525.
3. Long JA, Trinajstic K (2010) The Late Devonian Gogo Formation Lagerstatte of Western Australia: Exceptional early vertebrate preservation and diversity. *Annu Rev Earth Planet Sci* 38:255–279.
4. Morrow JR, Sandberg CA (2008) Evolution of Devonian carbonate-shelf margin, Nevada. *Geosphere* 4:445–458.
5. Zhu M, et al. (2009) The oldest articulated osteichthyan reveals mosaic gnathostome characters. *Nature* 458:469–474.
6. Coates MI (1999) Endocranial preservation of a Carboniferous actinopterygian from Lancashire, UK, and the interrelationships of primitive actinopterygians. *Phil Trans R Soc B* 354:435–462.
7. Dineley DL, Metcalf SJ (1999) *Fossil Fishes of Great Britain* (Joint Nature Conservation Committee, Peterborough).
8. Schaeffer B (1971) The braincase of the holostean fish *Macrepistius*, with comments on neurocranial ossification in the Actinopterygii. *Am Mus Novit* 2459:1–34.
9. Wood SP (1975) Recent discoveries of Carboniferous fishes in Edinburgh. *Scott J Geol* 11:251–258.
10. Menning M, Weyer D, Drozdzewski G, Van Amerom HWJ, Wendt I (2000) A Carboniferous timescale 2000: Discussion and use of geological parameters as time indicators from central and western Europe. *Geol Jahrb* A156:3–44.
11. Marshall CR (2008) A simple method for bracketing absolute divergence times on molecular phylogenies using multiple fossil calibration points. *Am Nat* 171:726–742.
12. Olsen PE (1984) The skull and pectoral girdle of the parasemionotid fish *Watsonulus eugnathoides* from the early Triassic Sakamena group of Madagascar, with comments on the relationships of the holostean fishes. *J. Vert. Paleo* 4:481–499.
13. Xu GH, Wu FX (2012) A deep-bodied ginglymodian fish from the Middle Triassic of eastern Yunnan Province, China, and the phylogeny of lower neopterygians. *Chin Sci Bull* 57:111–118.
14. Grande L, Bemis WE (1998) A comprehensive phylogenetic study of amiid fishes (Amiidae) based on comparative skeletal anatomy. An empirical search for interconnected patterns of natural history. *J Vert Paleo* 18(Memoir 4):1–690.
15. Catuneanu O, et al. (2005) The Karoo basins of south-central Africa. *J Afr Earth Sci* 43:211–253.
16. Ogg JG (2004) in *A Geologic Time Scale 2004*, eds Gradstein F, Ogg J, Smith A (Cambridge Univ Press, Cambridge), pp 271–306.
17. Xu GH, Gao KQ (2011) A new scanilepiform from the Lower Triassic of northern Gansu Province, China, and phylogenetic relationships of non-teleostean Actinopterygii. *Zool J Linn Soc* 161:595–612.
18. Hurley IA, et al. (2007) A new time-scale for ray-finned fish evolution. *Proc Biol Sci* 274:489–498.
19. Grande L, Jin F, Yabumoto Y, Bemis WE (2002) †*Protopsephurus liui*, a well-preserved primitive paddlefish (Acipenseriformes: polyodontidae) from the lower cretaceous of China. *J Vert Paleo* 22:209–237.

20. Hilton EJ, Forey PL (2009) Redescription of †*Chondrosteus acipenseroides* Egerton, 1858 (Acipenseriformes, †Chondrosteidae) from the Lower Lias of Lyme Regis (Dorset, England), with comments on the early evolution of sturgeons and paddlefishes. *J Syst Palaeontology* 7:427–453.
21. Swisher CC, et al. (2002) Further support for a Cretaceous age for the feathered-dinosaur beds of Liaoning, China: New Ar-40/Ar-39 dating of the Yixian and Tuchengzi formations. *Chin Sci Bull* 47:135–138.
22. Swisher CC, Wang YQ, Wang XL, Xu X, Wang Y (1999) Cretaceous age for the feathered dinosaurs of Liaoning, China. *Nature* 400:58–61.
23. Gardiner BG (1993) in *Fossil Record 2*, ed Benton MJ (Chapman and Hall, London), pp 611–619.
24. Forey PL (1997) A Cretaceous notopterid (Pisces: Osteoglossomorpha) from Morocco. *S Afr J Sci* 93:564–569.
25. Cavin L, Forey PL (2001) Osteology and systematic affinities of *Palaeonotopterus greenwoodi* Forey 1997 (Teleostei: Osteoglossomorpha). *Zool J Linn Soc* 133:25–52.
26. Taverne L, Maisey JG (1999) A notopterid skull (Teleostei, Osteoglossomorpha) from the continental Early Cretaceous of southern Morocco. *Am Mus Novit* 3260:1–12.
27. Sereno PC, et al. (1996) Predatory dinosaurs from the Sahara and Late Cretaceous faunal differentiation. *Science* 272:986–991.
28. Ogg JG, Agterberg FP, Grandstein FM (2004) in *A Geologic Time Scale 2004*, eds Gradstein F, Ogg J, Smith A (Cambridge Univ Press, Cambridge), pp 344–383.
29. Poyato-Ariza FJ (1996) in *Mesozoic Fishes-Systematics and Paleoecology*, eds Arratia G, Viohl G (Dr. Friedrich Pfeil, Munich), pp 319–328.
30. Poyato-Ariza FJ, Grande T (2010) in *Gonorynchiformes and Ostariophysian Relationships: A Comprehensive Review*, eds. Grande T, Poyato-Ariza FJ, Diogo R (Science, Enfield), pp 227–337.
31. Poyato-Ariza FJ (1996) in *Mesozoic Fishes-Systematics and Paleoecology*, eds Arratia G, Viohl G (Dr. Friedrich Pfeil, Munich), pp 329–348.
32. Poyato-Ariza FJ (1996) A revision of the ostariophysan fish family Chanidae, with special reference to the Mesozoic forms. *Paleo Ichth* 6:5–52.
33. Gratshev VG, Zherikhin VV (2000) New Early Cretaceous weevil taxa from Spain (Coleoptera, Curculionoidea). *Acta Geologica Hisp* 35:37–46.
34. Arratia G (1997) Basal teleosts and teleostean phylogeny. *Paleo Ichth* 7:5–168.
35. Lundberg JG (1975) Fossil catfishes of North America. *Papers in Paleontology, University of Michigan Museum of Paleontology* 11:1–51.
36. Lundberg JG (1992) in *Systematics, Historical Ecology, and North American Freshwater Fishes*, ed Mayden RL (Stanford Univ Press, Stanford, CA), pp 392–420.
37. Secord R, et al. (2006) Geochronology and mammalian biostratigraphy of middle and upper Paleocene continental strata, Bighorn Basin, Wyoming. *Am J Sci* 306:211–245.
38. Lundberg JG (1993) in *Biological Relationships Between Africa and South America*, ed Goldblatt P (Yale Univ Press, New Haven), pp 156–199.
39. Wilson MVH (1993) Calibration of Eocene varves at Horsefly, British Columbia, Canada, and temporal distribution of specimens of the Eocene fish *Amyzon aggregatum*. *Kaupia* 2:27–38.
40. Bruner JC (1991) Comments on the genus *Amyzon* (Family Catostomidae). *J Paleontol* 65:678–686.
41. Smith GR (1992) in *Systematics, Historical Ecology, and North American Freshwater Fishes*, ed Mayden RL (Stanford Univ Press, Stanford), pp 778–826.
42. Grande L, Eastman JT, Cavender TM (1982) *Amyzon gosiutensis*, a new catostomid fish from the Green River Formation. *Copeia* 1982:523–532.
43. Greenwood DR, Archibald SB, Mathewes RW, Moss PT (2005) Fossil biotas from the Okanagan Highlands, southern British Columbia and northeastern Washington State: Climates and ecosystems across an Eocene landscape. *Can J Earth Sci* 42:167–185.
44. Wolfe JA, Gregory-Wodzicki KM, Molnar P, Mustoe G (2003) Rapid uplift and then collapse in the Eocene of the Okanagan? Evidence from paleobotany. *Geological Association of Canada – Mineralogical Association of Canada – Society of Economic Geologists, Joint Annual Meeting*, (Vancouver, Canada) *Abstracts* 28:abstract 533.
45. Wilson MVH (1980) Oldest known *Esox* (Pisces: Esocidae) part of a new Paleocene teleost fauna from western Canada. *Can J Earth Sci* 17:307–312.
46. Wilson MVH, Brinkman DB, Neuman AG (1992) Cretaceous Esocoidei (Teleostei): Early radiation of the pikes in North American fresh waters. *J Paleontol* 66:839–846.
47. Eberth DA, Braman DR (1993) Selected Upper Cretaceous section of the southern Alberta Plains: the Judith River Group, Horseshoe Canyon Formation, Whitemud, Battle and the Scollard formations, and the Cretaceous-Tertiary boundary. (Edmonton, Canada) in *Geological Society of Canada Joint Annual Meeting 1993, Field Trip B-2 Guidebook, Edmonton, Alberta*:1–84.
48. Wilson MVH, Li GQ (1999) Osteology and systematic position of the Eocene salmonid *Eosalmo driftwoodensis* Wilson from western North America. *Zool J Linn Soc* 125:279–311.
49. Greenwood DR, Archibald SB, Mathewes RW, Moss PT (2005) Fossil biotas from the Okanagan Highlands, southern British Columbia and northeastern Washington State: Climates and ecosystems across an Eocene landscape. *Can J Earth Sci* 42: 167–185.
50. Patterson C (1964) A review of Mesozoic acanthopterygian fishes, with special reference to those of the English Chalk. *Phil. Trans. R. Soc. B* 247:213–482.
51. Patterson C (1993) An overview of the early fossil record of acanthomorphs. *Bull Mar Sci* 52:29–59.
52. Owen E (1987) in *Fossils of the Chalk. Palaeontological Association Field Guides to Fossils: Number 2*, ed Smith AB (Oxford Univ Press, Oxford), pp 9–14.
53. Rosen DE (1973) in *Interrelationships of Fishes*, eds Greenwood PH, Miles RS, Patterson C (Academic, London), pp 397–513.
54. Murray AM (1996) A new Paleocene genus and species of percopsid, †*Massamorichthys wilsoni* (Paracanthopterygii) from Joffre Bridge, Alberta, Canada. *J Vert Paleo* 16: 642–652.
55. Murray AM, Wilson MVH (1999) in *Mesozoic Fishes 2—Systematics and Fossil Record*, eds Arratia G, Schultze H-P (Dr. Friedrich Pfeil, Munich), pp 397–411.
56. Fox RC (1990) The succession of Paleocene mammals in western Canada. *Spec Pap Geol Soc Am* 243:51–70.
57. Rosen DE, Patterson C (1969) The structure and relationships of the paracanthopterygian fishes. *Bull Am Mus Nat Hist* 141:357–474.
58. Evanoff E, McIntosh WC, Murphey PC (2001) Stratigraphic summary and 40Ar/39Ar geochronology of the Florissant Formation, Colorado. *Proceedings of the Denver Museum of Nature and Science* Series 4, no. 1:1–16.
59. Tyler JC, Bronzi P, Ghiandoni A (2000) The Cretaceous fishes of Nardò. 11°. A new genus and species of Zeiformes, *Cretazeus rinaldii*, the earliest record for the order. *Boll Museo Civico di Storia Naturale di Verona* 24:11–28.
60. Tyler JC, Santini F (2005) A phylogeny of the fossil and extant zeiform-like fishes, Upper Cretaceous to Recent, with comments on the putative zeomorph clade (Acanthomorpha). *Zool Scr* 34:157–175.
61. Danil'chenko PG (1960) Kostistye ryby Maikopskikh otlozhenii Kavkaza. *Trudy Paleon Inst* 78:1–208.
62. Baciu D-S, Bannikov AF, Tyler JC (2005) Revision of the fossil fishes of the family Zeidae (Zeiformes). *Boll Mus Storia Nat Verona Geol Paleon Preist* 29:95–128.
63. Santini F, Tyler JC, Bannikov AF, Baciu DS (2006) A phylogeny of extant and fossil buckler dory fishes, family Zeidae (Zeiformes, Acanthomorpha). *Cybium* 30:99–107.
64. Jones RW, Simmons MD (1997) A review of the stratigraphy of Eastern Paratethys (Oligocene-Holocene), with particular emphasis on the Black Sea. *AAPG Mem* 68:39–52.
65. Luterbacher HP, et al. (2004) in *A Geologic Time Scale 2004*, eds Gradstein F, Ogg J, Smith A (Cambridge Univ Press, Cambridge), pp 384–408.
66. Danil'chenko PG (1968) in *Outlines on the Phylogeny and Systematics of Fossil Fishes and Agnathans* (in Russian), ed Obruchev DV (Nauka, Moscow), pp 113–156.
67. Bannikov AF (1999) Review of fossil Lampridiformes (Teleostei) finds with a description of a new Lophotidae genus and species from the Oligocene of the northern Caucasus. *Paleontol J* 33:68–76.
68. Bannikov AF, Parin NN (1997) The list of marine fishes from Cenozoic (Upper Paleocene-middle Miocene) localities in southern European Russia and adjacent countries. *J Ichthyol* 37:150–155.
69. Sorbini C, Sorbini L (1999) The Cretaceous fishes of Nardo. 10: *Nardovelifer altipinnis*, gen. et sp. nov. (Teleostei, Lampridiformes, Veliferidae). *St Ric Giac Terz Bolca* 8: 11–27.
70. Wiley EO, Johnson GD, Dimmick WW (1998) The phylogenetic relationships of lampridiform fishes (Teleostei: acanthomorpha), based on a total-evidence analysis of morphological and molecular data. *Mol Phylogenet Evol* 10:417–425.
71. Olney JE, Johnson GD, Baldwin CC (1993) Phylogeny of lampridiform fishes. *Bull Mar Sci* 52:137–169.
72. Bown PR (2001) Calcareous nannofossils of the Gault, Upper Greensand and Glauconitic Marl (Middle Albian-Lower Cenomanian) from the BGS Selborne boreholes, Hampshire. *Proc Geol Assoc* 112:223–236.
73. Sorbini L (1979) The Holocentridae of Monte Bolca. III. *Berybolcensis leptacanthus* (Agassiz). *Stud Ric Giaciam Terz Bolca* 4:19–35.
74. Sorbini L (1975) The Holocentridae of Monte Bolca. I: *Eoholocentrum*, nov. gen., *Eoholocentrum macrocephalum* (de Blainville) (Pisces-Actinopterygii). *Stud Ric Giaciam Terz Bolca* 2:205–228.
75. Sorbini L (1975) The Holocentridae of Monte Bolca. II: *Tenuicentrum pattersoni* nov. gen. nov. sp. Nuovi dati a favoure dell'origine monofiletica dei beryciformi (Pisces). *Stud Ric Giaciam Terz Bolca* 2:456–472.
76. Stewart JD (1984) Taxonomy, paleoecology, and stratigraphy of the halecostome-inoceramid associations of the North American Upper Cretaceous epicontinental seaways. PhD thesis (Univ of Kansas, Lawrence, KS).
77. Papazzoni CA, Trevisani E (2006) Facies analysis, palaeoenvironmental reconstruction, and biostratigraphy of the "Pesciara di Bolca" (Verona, northern Italy): An early Eocene *Fossil-Lagerstätte*. *Palaeogeogr Palaeoclimat Palaecol* 242:21–35.
78. Moore JA (1993) Phylogeny of the Trachichthyiformes (Teleostei: Percomorpha). *Bull Mar Sci* 52:114–136.
79. Zehren SJ (1979) The comparative osteology and phylogeny of the Beryciformes. *Ecol Monogr* 1:1–389.
80. Sorbini L (1981) The Cretaceous fishes of Nardò. I°. Order Gasterosteiformes (Pisces). *Boll Museo Civico di Storia Naturale di Verona* 8:1–27.
81. Orr JW (1995) Phylogenetic relationships of the gasterosteiform fishes (Teleostei: Acanthomorpha). PhD thesis (Univ of Washington, Seattle, WA), p 813.
82. Pietsch TW (1978) Evolutionary relationships of the sea moths (Teleostei: Pegasidae) with a classification of the gasterosteiform families. *Copeia* 1978:517–529.
83. Medizza F, Sorbini L (1980) in *I Vertebrati Fossili Italiani—Catalogo dell Mostra* (Museo Civico di Storia Naturale, Verona), pp 131–134.
84. Blot J (1980) The ichthyofauna of the deposits of Monte Bolca (Province de Vérone, Italie). Catalogue systématique présentat l'état actuel des recherches concernant cette faune. *Bull Mus nation d'Hist nat, Paris*, 4e serie, sec. C 2:339–396.
85. Smith-Vaniz WF (1984) in *Ontogeny and Systematics of Fishes*, eds. Moser HG, et al. (Allen Press, Lawrence, KS), pp 522–530.
86. Wettstein A (1886) On the fish fauna of the Tertiary Glarner slate. *Abh Schweiz Paläon Ges* 13:1–103.
87. Micklich NR (1998) New information on the fish fauna of the Frauenweiler fossil site. *Ital J Zool (Modena)* 65(Supp. 1):169–184.
88. O'Toole B (2002) Phylogeny of the species of the superfamily Echeneoidea (Perciformes: Carangoidei: Echeneidae, Rachycentridae, and Coryphaenidae), with an interpretation of echeneid hitchhiking behaviour. *Can J Zool* 80:596–623.
89. Johnson GD (1984) in *Ontogeny and Systematics of Fishes*, eds. Moser HG, et al. (Allen Press, Lawrence, KS), pp 464–498.
90. Gasser D, den Brok B (2008) Tectonic evolution of the Engi Slates, Glarus Alps, Switzerland. *Swiss J Geosci* 101:311–312.

91. Fischer H, Villa I (1990) Erste First K-Ar and $^{40}Ar/^{39}Ar$ hornblende mineral ages of the Taveyannaz sandstones. *Schweis Mineral. Petrograph Mitteil* 70:73–75.
92. Micklich NR, Tyler JC, Johnson GD, Swidnicka E, Bannikov AF (2009) First fossil records of the tholichthys larval stage of butterfly fishes (Perciformes, Chaetodontidae), from the Oligocene of Europe. *Palaontol. Z* 83:479–497.
93. Bannikov AF, Tyler JC (1995) Phylogenetic revision of the fish families Luvaridae and †Kushlukiidae (Acanthuroidei), with a new genus and two new species of Eocene luvarids. *Smithson Contrib Paleobiol* 81:1–45.
94. Tyler JC, Bannikov AF (1997) Relationships of the fossil and recent genera of rabbitfishes (Acanthuroidei: Siganidae). *Smithson Contrib Paleobiol* 84:1–35.
95. Friedman M (2008) The evolutionary origin of flatfish asymmetry. *Nature* 454: 209–212.
96. Chanet B (1997) A cladistic reappraisal of the fossil flatfishes record consequences on the phylogeny of the Pleuronectiformes (Osteichthyes: Teleostei). *Ann Sci nat, Zool, Paris 13e Sér*. 18:105–117.
97. Chanet B (1994) *Eubuglossus eocenicus* (Woodward 1910) from the Upper Lutetian of Egypt, one of the oldest soleids (Teleostei, Pleuronectiformes). *Neu Jahrbuch Geolo Paläon Monatshefte* 1994:391–398.
98. Chapleau F (1988) Comparative osteology and intergeneric relationships of the tongue soles (Pisces, Pleuronectiformes, Cynoglossidae). *Can J Zool* 66:1214–1232.
99. Baciu DS, Chanet B (2002) The fossil flatfishes (Teleostei: Pleuronectiformes) from the Oligocene of Piatra Neamt (Romania). *Oryctos* 4:17–38.
100. Carnevale G (2006) Morphology and biology of the Miocene butterflyfish *Chaetodon ficheuri* (Teleostei: Chaetodontidae). *Zool J Linn Soc* 146:251–267.
101. Blum SD (1988) The osteology and phylogeny of the Chaetodontidae (Teleostei: Perciformes). PhD thesis (Univ of Hawaii, Honolulu), p 365.
102. Krijgsman W, Hilgen FJ, Raffi I, Sierro FJ, Wilson DS (1999) Chronology, causes and progression of the Messinian salinity crisis. *Nature* 400:652–655.
103. Hilgen FJ, et al. (1995) Extending the astronomical (polarity) time scale into the Miocene. *Earth Planet Sci Lett* 136:495–510.
104. Carnevale G (2004) The first fossil ribbonfish (Teleostei, Lampridiformes, Trachipteridae). *Geol Mag* 141:573–582.
105. Yabumoto Y, Uyeno T (2011) *Euleiognathus*, a new genus proposed for the Miocene ponyfish, *Leiognathus tottori* Yabumoto and Uyeno 1994 (Perciformes: Leiognathidae) from Japan. *Ichthyol Res* 58:19–23.
106. Yabumoto Y, Uyeno T (1994) A new Miocene ponyfish of the genus *Leiognathus* (Pisces, Leiognathidae). *Bull Nat Sci Mus Tokyo Ser C* 20:67–77.
107. Chakrabarty P, Sparks JS (2008) Diagnoses for *Leiognathus* Lacepede 1802, *Equula* Cuvier 1815, *Equulites* Fowler 1904, *Eubleekeria* Fowler 1904, and a new ponyfish genus (Teleostei: Leiognathidae). *Am Mus Novit* 3623:1–11.
108. Yamashita T, Kimura S (2001) A new species, *Gazza squamiventralis*, from the East Coast of Africa (Perciformes: Leiognathidae). *Ichthyol Res* 48:161–166.
109. Sparks JS, Dunlap PV, Smith WL (2005) Evolution and diversification of a sexually dimorphic luminescent system in ponyfishes (Teleostei: Leiognathidae), including diagnoses for two new genera. *Cladistics* 21:305–327.
110. Lourens L, Hilgen F, Shackleton NJ, Laskar J, Wilson D (2004) in *A Geologic Time Scale 2004*, eds Gradstein F, Ogg J, Smith A (Cambridge Univ Press, Cambridge), pp 409–440.
111. Santini F, Tyler JC (2003) A phylogeny of the families of fossil and extant tetraodontiform fishes (Acanthomorpha, Tetraodontiformes), Upper Cretaceous to recent. *Zool J Linn Soc* 139:565–617.
112. Tyler JC, Santini F (2002) Review and reconstructions of the tetraodontiform fishes from the Eocene of Monte Bolca, Italy, with comments on related Tertiary taxa. *Museo Civico di Storia Naturale di Verona* 9:47–119.
113. Bannikov AF, Tyler JC (2008) A new genus and species of triggerfish from the Middle Eocene of the northern Caucasus, the earliest member of the Balistidae (Tetraodontiformes). *Paleontol. J* 42:615–620.
114. Smith GR, Miller RR (1985) in *Late Cenozoic History of the Pacific Northwest*, ed Smiley CJ (American Association for the Advancement of Science, San Francisco), pp 75–83.
115. Smith GR, Elder RL (1985) in *Late Cenozoic History of the Pacific Northwest*, ed. Smiley CJ (American Association for the Advancement of Science, San Fransisco), pp 85–93.
116. Smith GR (1975) Fishes of the Pliocene Glenns Ferry Formation, southwestern Idaho. *Papers in Paleontology, University of Michigan Museum of Paleontology* 14: 1–68.
117. Wing SL (1998) in *Evolution of Tertiary Mammals of North America*, eds Janis CM, Scott KM, Jacobs LL (Cambridge Univ Press, Cambridge), Vol 1, pp 37–65.
118. Graham A (1999) *Late Cretaceous and Cenozoic History of North American Vegetation* (Oxford Univ Press, Oxford).

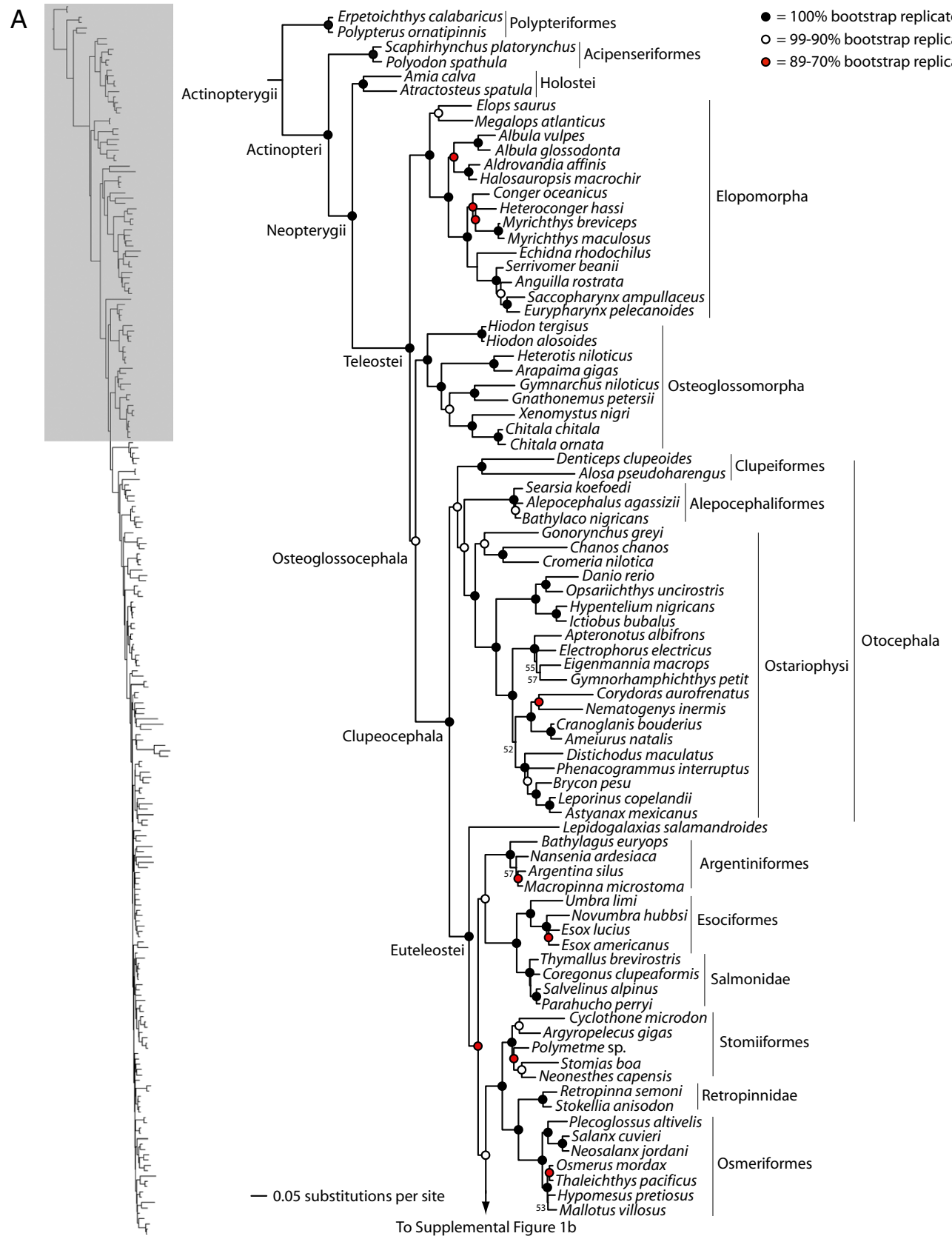

Fig. S1. (Continued)

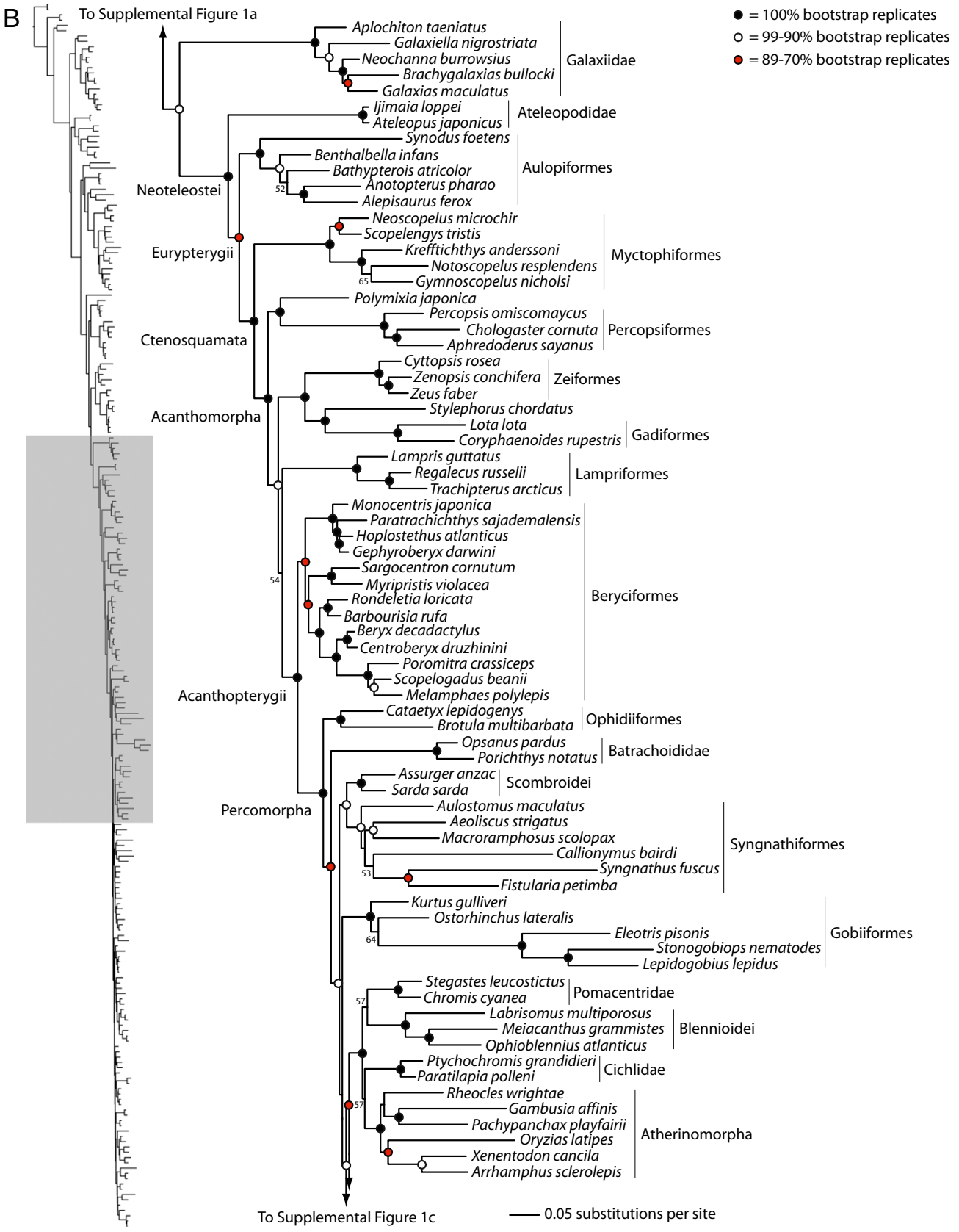

Fig. S1. (Continued)

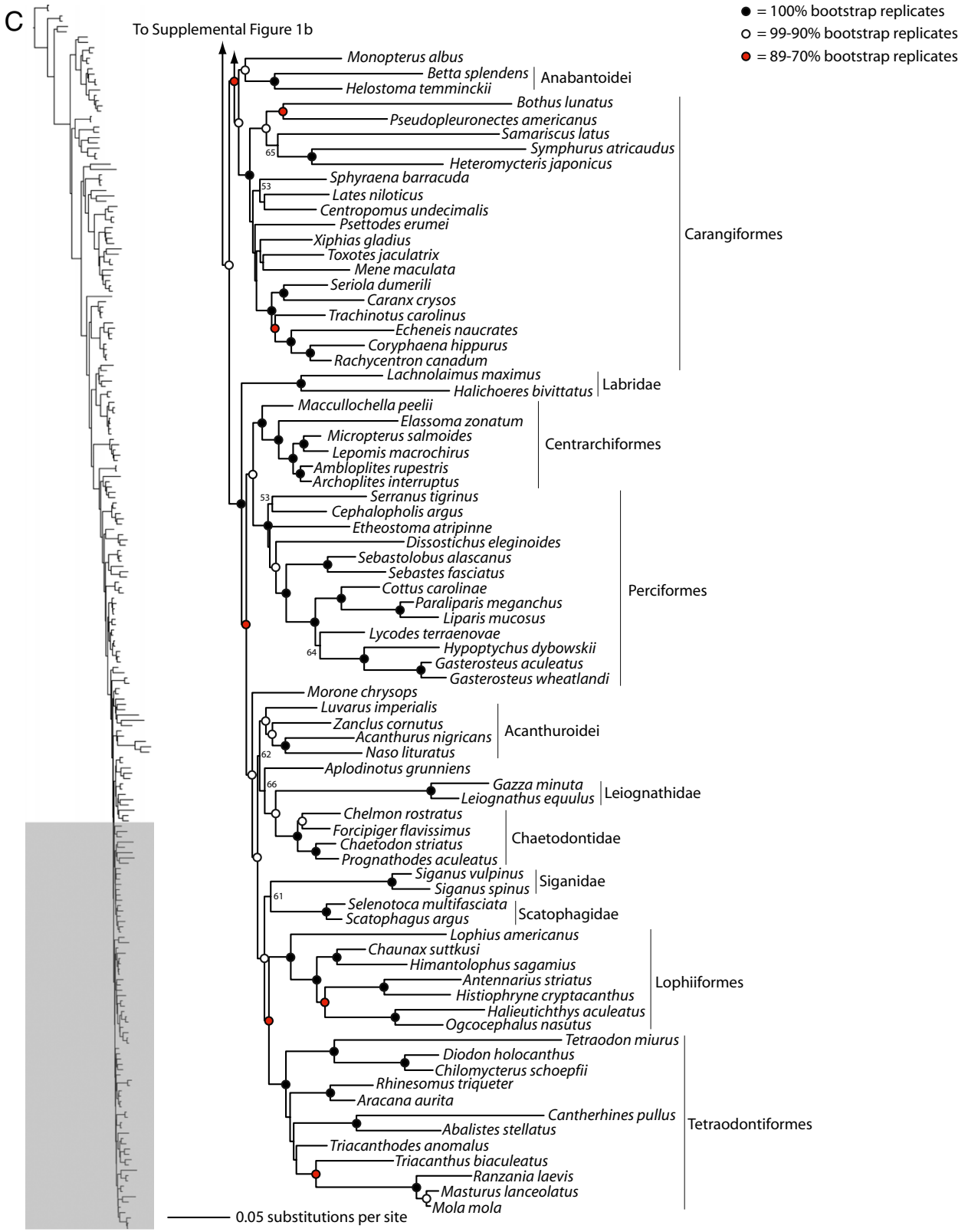

Fig. S1. Phylogeny of 232 actinopterygian species inferred from a partitioned maximum-likelihood analysis of nine nuclear genes. Filled black circles identify clades supported with a bootstrap score of 100%, unfilled circles identify clades supported with a bootstrap score between 99% and 90%, and filled red circles identify clades supported with a bootstrap score between 89% and 70%. The shaded portion of the phylogeny along the side of the figure indicates placement of clades in the full actinopterygian phylogeny. Major clades are indicated and the phylogeny is presented in three parts, labeled (*A*), (*B*), and (*C*).

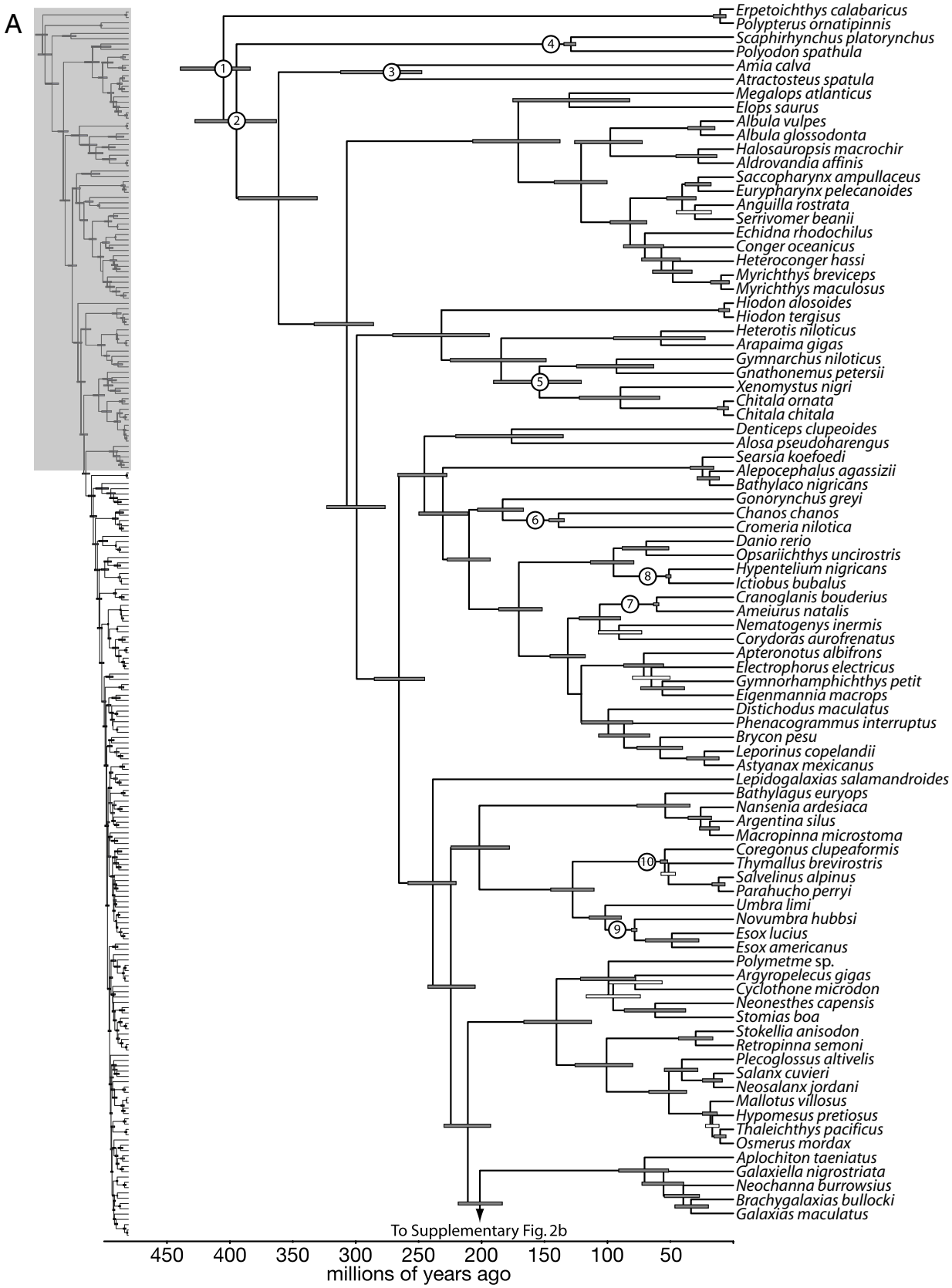

Fig. S2. (Continued)

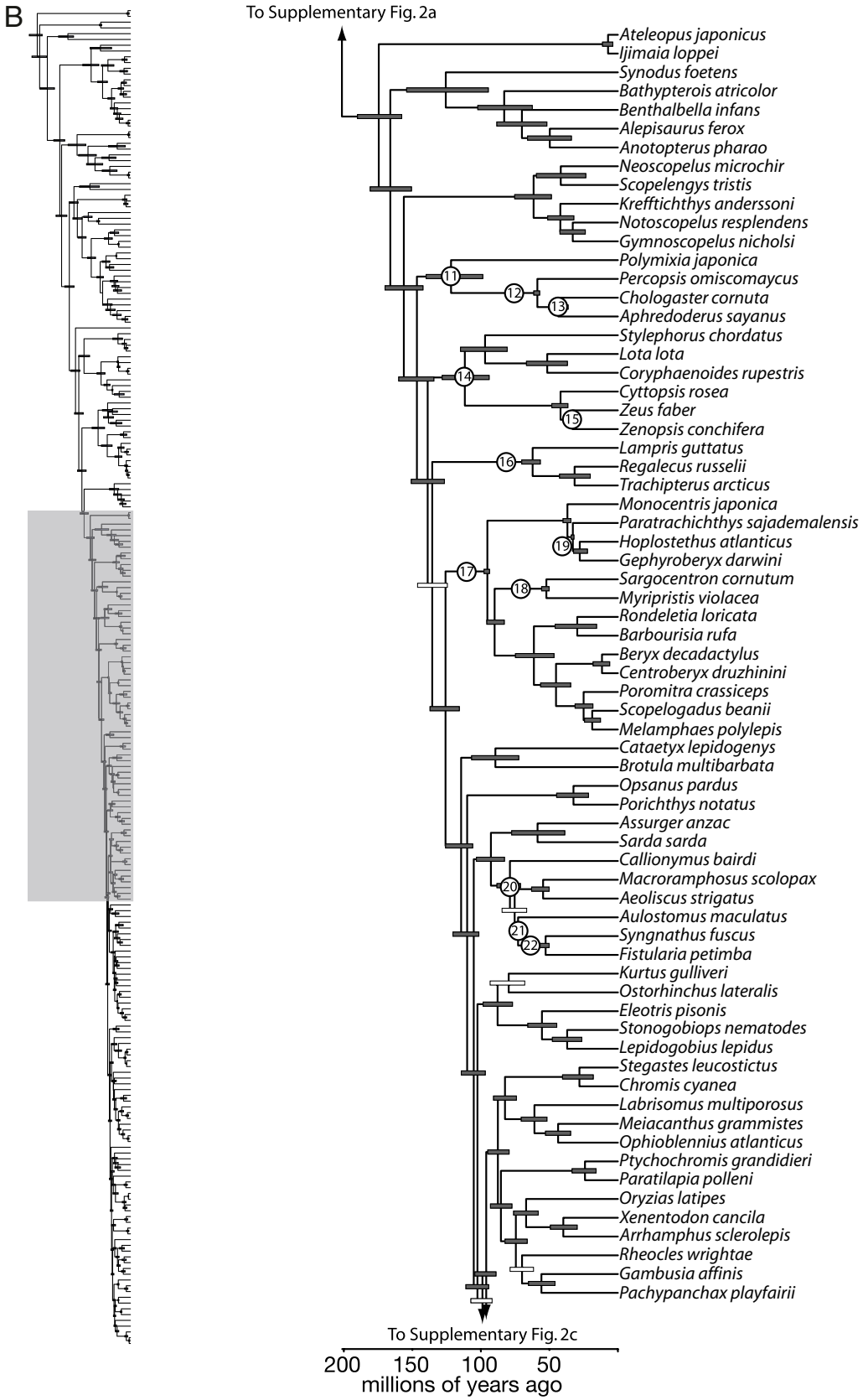

Fig. S2. (Continued)

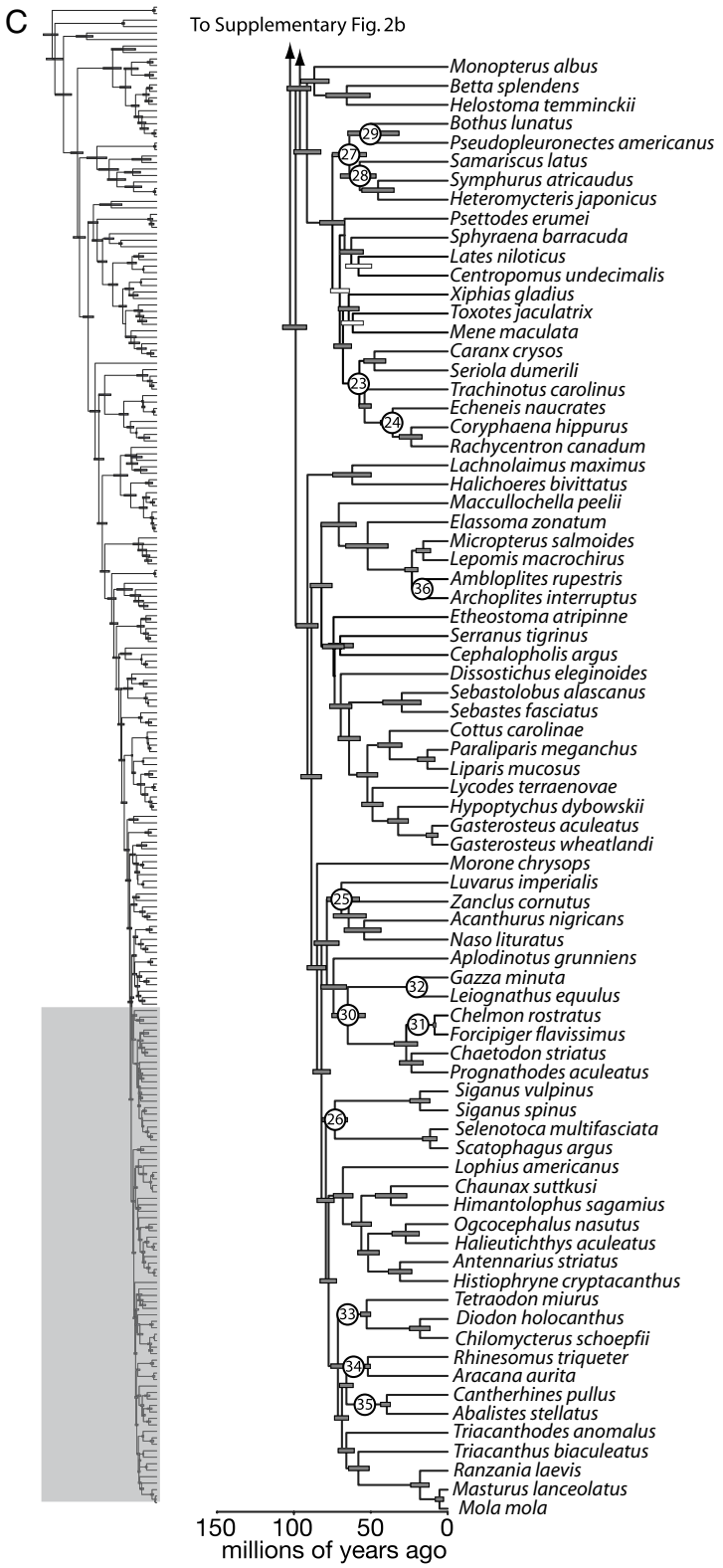

Fig. S2. Fully annotated Actinopterygian time-calibrated phylogeny chronogram based on nine nuclear genes and 36 fossil age constraints. Bars represent the posterior distribution of divergence time estimates. Gray bars identify nodes supported with Bayesian posterior probabilities (BPP) ≥ 0.95, and white bars mark nodes with BPP < 0.95. Nodes with age priors taken from the fossil record are numbered and specific information on calibrations are given in the *SI Text*. Calibration labels are placed on the branch leading to the node if it would completely obscure the bar depicting the posterior distribution. The time-calibrated tree is scaled to the geological time scale with absolute time given in millions of years. The shaded portion of the phylogeny along the side of the figure indicates placement of clades in the full actinopterygian phylogeny. The time-calibrated phylogeny is presented in three parts, labeled (*A*), (*B*), and (*C*).

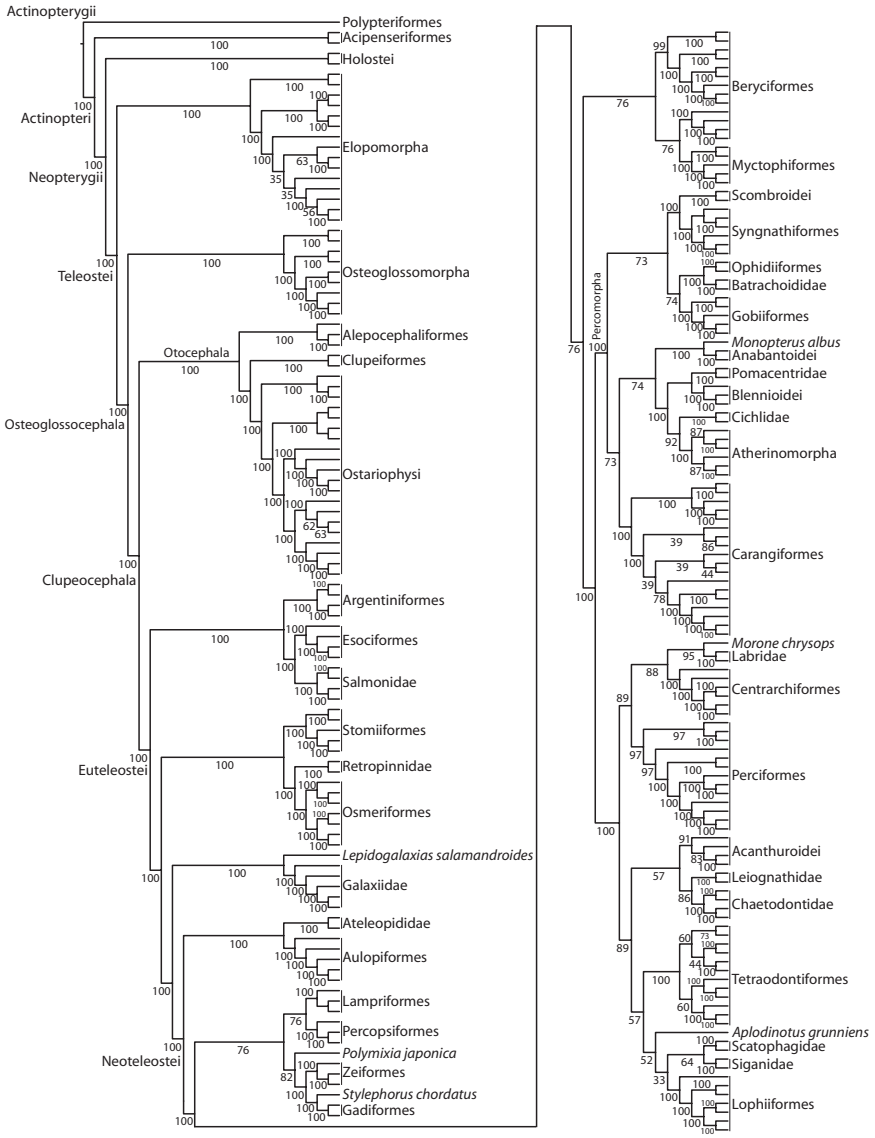

Fig. S3. Species tree phylogeny of 232 actinopterygian species inferred using gene tree parsimony. Bootstrap values are given at nodes. Major actinopterygian clades are labeled.

Other Supporting Information Files

Table S1 (DOC)
Table S2 (DOC)